International Journal of Informatics Society

03/23 Vol. 14 No. ISSN 1883-4566

Informatics Society

Aims and Scope

The purpose of this journal is to provide an open forum to publish high quality research papers in the areas of informatics and related fields to promote the exchange of research ideas, experiences and results.

Informatics is the systematic study of Information and the application of research methods to study Information systems and services. It deals primarily with human aspects of information, such as its qu ality and value as a resource. Informatics also referred to as Information science, studies t he structure, algorithms, behavior, and interactions of natural and a rtificial systems that store, process, access and communicate information. It also develops its own conceptual and theoretical foundations and utilizes foundations developed in other fields. The advent of computers, its ubiquity and ease to use has led to th e study of info rmatics that has computational, cognitive and social aspects, including study of the social impact of information technologies.

The characteristic of informatics' context is amalgamation of technologies. For creating an informatics product, it is necessary to integrate many technologies, such as mathematics, linguistics, engineering and other emerging new fields.

Guest Editor's Message

Shinji Kitagami
Guest Editor of the Forty-second Issue of the International Journal of Informatics Society

We are delighted to have the Forty-second issue of the International Journal of Informatics Society (IJIS) published. This issue includes selected papers from the Fifteenth International Workshop on Informatics (IWIN2021), which was held online, Sept. 12-13, 2021. The workshop was the fifteenth event for the Informatics Society, and was intended to bring together researchers and practitioners to share and exchange their experiences, discuss challenges and present original ideas in all aspects of informatics and computer networks. In the workshop, 29 papers were presented in seven technical sessions. The workshop was successfully finished with precious experiences provided to the participants. It highlighted the latest research results in the area of informatics and its applications that include networking, mobile ubiquitous systems, data analytics, business systems, education systems, design methodology, intelligent systems, groupware, and social systems.

Each paper submitted to IWIN2021 was reviewed in terms of technical content, scientific rigor, novelty, originality, and quality of presentation by at least two reviewers. Through those reviews, 19 papers were selected for publication candidates of IJIS Journal, and they were further reviewed as a Journal paper. We have three categories of IJIS papers, Regular papers, Industrial papers, and Invited papers, each of which was reviewed from different points of view. This volume includes papers among those accepted papers, which have been improved through the workshop discussion and the reviewers' comments.

We publish the journal in print as well as in an electronic form over the Internet. We hope that the issue would be of interest to many researchers as well as engineers and practitioners over the world.

Shinji Kitagami is a Professor of Department of Management and Information Sciences, Faculty of Environment and Information Sciences at Fukui University of Technology since 2017. He joined Mitsubishi Electric Corporation in 1983. He received his Ph.D. degree in Information Sciences from Tohoku University in 2013. He has been engaged in research and development of Broadband Internet Services, Energy Management Systems for commercial building and factory, IoT Architecture, IoT Networks, and Method of IoT Human Resource Development. He received Best Paper Awards from FA (Factory Automation) Foundation in 2017. He is a member of IPSJ, IEICE, IEEJ and JSEE (Japanese Society for Engineering Education).

Industry Paper

Quantitative Process Improvement for Progress Management Process

†Akihiro Hayashi

†Department of Information Design, Shizuoka Institute of Science and Technology, Japan
pixysbrain@gmail.com

Abstract - The concept of process improvement in system development is applied to prevent rework in downstream processes by correctly defining requirements and communication in upstream processes. Although rework related to the entire project life cycle has been discussed thus far, it is necessary to improve each process individually. In this study, we focused on the progress management process, which is most frequently used in the development life cycle. First, we defined the workload as the basis of progress management. We also estimated the project workload in different ways during the project planning stage. The workload delay of the project can be controlled by introducing an earned value management approach to project progress management. The necessary corrective actions were taken. Upon completion of the project, we aimed to improve the estimation accuracy by accumulating workload data as an organization. When this proposed method was applied to a company that achieved Capability Maturity Model IntegrationCMMI level 3, an actual improvement in the accuracy of workload estimation was confirmed.

Keywords: Process Improvement, Progress Management, EVM

1 INTRODUCTION

Process improvement in system development has been widely discussed since the release of the software Capability Maturity Model (CMM) Ver1.1 in 1993. The main idea was to accurately define the requirements in the upstream process and accurately estimate the scale and construction period of the project, thereby eliminating any delays in the downstream process. As a basis for this, a graph was presented showing that if modification occurred in the coding stage of the project life cycle, the modification cost would be less than half in the upstream process; however, if modification occurred in the downstream process, it would increase exponentially. It is important to manage the upstream processes to prevent this type of retrogression.

In this study, focusing on the most frequently used progress management process in system development, we propose process improvement. Progress management is the process of measuring the progress of a project according to the project plan and correcting any discrepancies. The progress management process is basically implemented at the progress meetings. Progress meetings are held weekly in many companies. In some industries, it is common to hold progress meetings every morning. Thus, we can expect to enhance the process through the improvement of the productivity of the progress management process by reducing rework, as well as the time and effort required for progress meetings.

First, we review Capability Maturity Model Integration (CMMI)'s progress management practices and highlight the deficiencies in managing progress. Thereafter, using effort as the basis, we propose a method for estimating the effort of the project, evaluating the progress of the project, and estimating the cost overruns upon project completion. We aim to spiral up by registering the knowledge acquired after the project is completed in the organization's process assets and reflect it in the estimate of the next project plan.

In a prior study in the process improvement field, Mayra Proano-Narvaez et al . [1] evaluated the effectiveness of project management using Earned Value Management (EVM) using the case of a construction company in Cuenca . They reported that EVM plays an essential role in the integrated management of projects in terms of scope, time, and cost. However, this study was not a system development project and did not discuss quantitative progress management. Guoping Rong et al. [2] pointed out that CMMI, which has been validated in the traditional software industry paradigm, has not been evaluated in a DevOps environment. Therefore, we evaluated the application of process improvement using SCAMPI C in an actual DevOps case. As a result, we report that SCAMPI C can be introduced to process improvements in DevOps. Rojrattanakorn et al. [5] pointed out that despite the importance of risk management in software development projects, it is still judged subjectively. In their study, they proposed a method to identify risks using risk taxonomy ontology and CMMI's project planning guidelines. The study reported that this method was effective for the risk management of software projects.

Furthermore, prior research on process improvement and progress management has been reported([3][4][6]), but no research reports how to manage progress consistently from project planning to project completion.

In Section 2, we outline the CMMI progress management process, pointing out the lack of progress management practices and problems to be solved. In Section 3, we propose a method of project progress management for master schedule and work breakdown structure (WBS), and a method of progress management based on man-hours by EVM. Section 4 discusses the results of the application of this proposal to actual projects. In Section 5, we discuss the results, and the conclusions are presented in Section 6.

2 PRACTICE AND ISSUES REQUIRED FOR PROGRESS MANAGEMENT

2.1 CMMI Progress Management Process and Management Items

In CMMI, the most standard process management model currently being used, the equivalent of progress management is project monitoring and control, as shown in Fig.1. This process describes the following goals and practices:

Here, SG1 (goal 1) lists the management items for each progress meeting, and SG2 (goal 2) lists the management items for issues and corrective actions. In other words, SG1 is described as "weekly management items" and SG2 is described as "weeks-long management items." In other words, the progress management practices described in CMMI are intended for progress meetings, which are the main areas of progress management.

2.2 Issues to Be Solved

Notably, CMMI and other so-called best practices describe what to do but not how to do it. Organizations that achieve CMMI level 3 may have successfully introduced the progress management process at that point, but it is debatable whether this specifically improves the progress management process. Adopting a best practice model to implement progress management has not yet been able to establish a methodology that contributes to the overall productivity of the project, and it remains a challenge to be solved.

2.3 Identify Deficiencies in The Progress Management Process

In this study, we conducted a case analysis of progress management in the organizations wherein the author worked. Below is an outline of each organization's efforts.

A: NTT 's affiliates are developing prototypes of basic research. They are working to improve the process by introducing the CMMI software as soon as possible in Japan.

B: As a foreign computer manufacturer, we are strong in large-scale development. We have a unique software development lifecycle and implement project management using global standards.

C: A company that manufactures precision equipment for automobiles; we are proceeding with the improvement of internal processes while sticking to standards and mechanisms, such as CMMI and ISO9001, according to the management's preferences.

D: An IT development company of a major steel manufacturer; we are implementing in-house process improvements using ISO/IEC 15504. We recommend strict procedures for system development.

SG 1 Monitor the Project Against the Plan
SP 1.1 Monitor Project Planning Parameters
SP 1.2 Monitor Commitments
SP 1.3 Monitor Project Risks
SP 1.4 Monitor Data Management
SP 1.5 Monitor Stakeholder Involvement
SP 1.6 Conduct Progress Reviews
SP 1.7 Conduct Milestone Reviews
SG 2 Manage Corrective Action to Closure
SP 2.1 Analyze Issues
SP 2.2 Take Corrective Action
SP 2.3 Manage Corrective Actions

Figure 1: Project monitor and control

Based on the experience with these four organizations and documents such as shared consultation materials and session minutes left in the cloud environment, a fishbone diagram, as shown in Fig.2, was created to identify the factors lacking in the progress management process.

Fishbone diagrams can be used in two ways: organizing and reviewing. Here, the fishbone diagram was used for the purpose of organization. When there are too many factors, each factor is systematically organized by dividing it into common elements and levels of abstraction. In this study, four factors involved in this research were identified by creating a fishbone diagram.

According to the results, four main factors make the progress management process incomplete.

1. Absence of project baselines (Factor 1)
   No key measures have been defined for overall project progress management, and there is a lack of project baselines to serve as milestones for the creation of deliverables.

2. Feasibility has not been assessed (Factor 2)
   The feasibility of creating a correct master schedule and WBS and completing the project on time from a man-hour perspective has not been evaluated based on the evaluation of both top-down and bottom-up.

3. Lack of skills related to WBS (Factor 3)
   WBS does not function as a baseline, even though WBS is being created, the WBS code is not defined correctly, and the WBS dictionary is formally written with the start and end dates.

4. Lack of cost progress measures (Factor 4)
   In the development phase, reliable costs have not been calculated and are being calculated. To meet deadlines, costs are secondary, while cost consciousness is low.

3 QUANTITATIVE PROCESS IMPROVEMENT FOR PROGRESS MANAGEMENT PROCESS

In Section 3, to solve the problems presented in Section 2, we propose a method for continuous improvement of the progress management process. We present the basic policy of this study and comprehensively explain the proposed method.

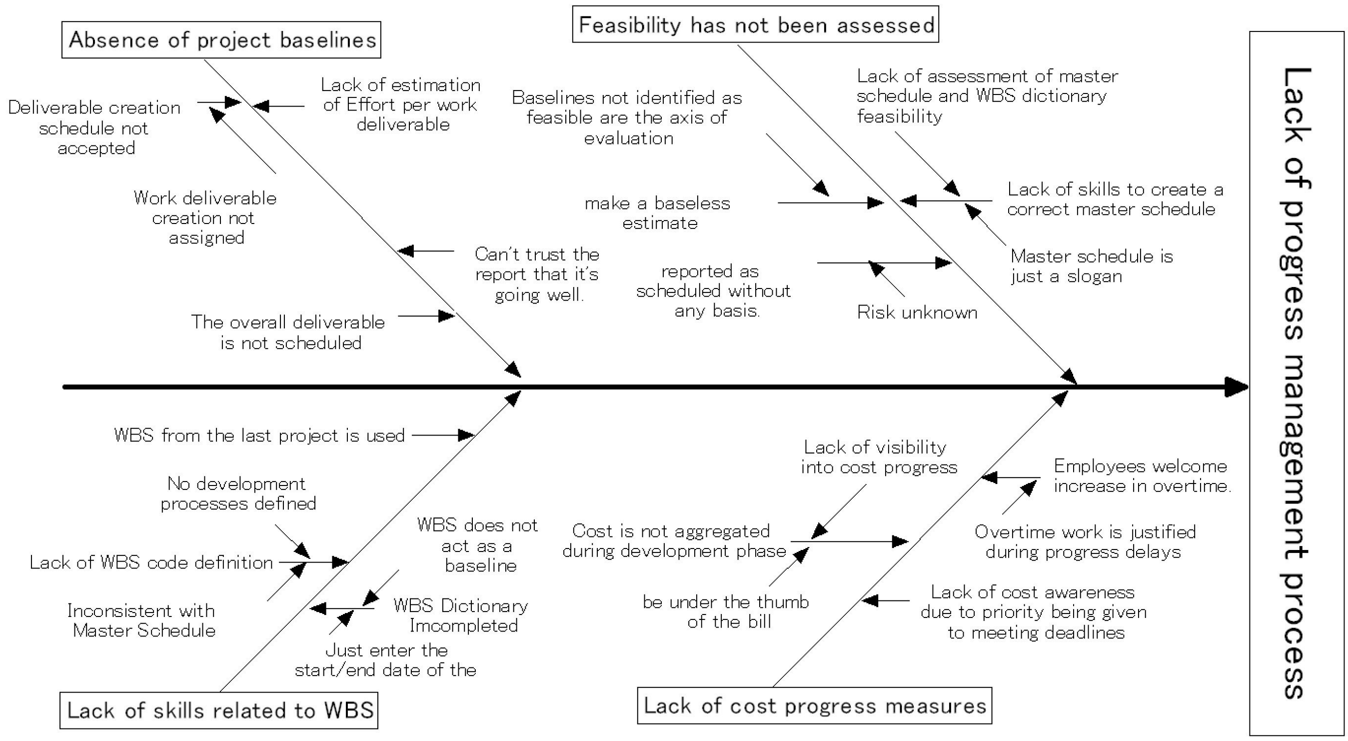

Figure 2: Insufficient factor of progress management

3.1 Basic Policy

The key to successful project management is creating a feasible project plan, operating the project in accordance with the plan, and adapting to the changes and risks that occur in the middle of the project. In this study, effort was considered the key parameter and basis of progress management.

At the project planning stage, the effort and construction period of the new system are estimated using several methods, and the master schedule and WBS are created using the effort as the axis. Thereafter, progress reports and risk assessments are made using EVM based on the effort. Upon completion of the project, the relationship between the characteristics of the project and effort is registered in the organization's process assets and utilized in the next project, aiming to spiral up progress management based on effort. This method solves for the four factors shown in the fishBone diagram. This situation is illustrated in Fig. 3.

3.2 Project Planning

3.2.1 Effort and Period Estimation

We define the requirements in the most detailed way possible to start a project and use the source lines of code (SLOC) as the scale of the new system. In this study, we do not discuss the method of scale estimation using SLOC; we use top-down and bottom-up approaches to estimate the effort.

Table 1: Effort Estimation Adjustment

Top Down Approach	Conversion to Effort using the CoBRA method
Bottom Up Approach	Calculation of Effort by stacking WBS

The top-down approach refers to the CoBRA method that converts SLOCs into effort. CoBRA is an estimation method that visualizes a "guess." For example, it quantifies user experience values, such as user communication, level of performance requirements, ambiguity of requirements, and system complexity as risks of system development. The effectiveness of the CoBRA method has been confirmed in many previous studies [7][8].

The bottom-up approach to man-hour estimation refers to the accumulation of man-hours required to create work deliverables described in the WBS.

The bottom-up approach to effort estimation refers to accumulation of the effort required to create work deliverables described in the WBS. For an organization that introduces CMMI, a configuration management plan is prepared at the time of project planning, and the work output (including source code) and number created for each process are identified and assigned to the person in charge. If a person takes five days to produce a work deliverable, it takes 50 days to produce ten work deliverables. By accumulating the effort created for each process, the overall effort of the project is determined from the bottom up.

The effort obtained by the top-down approach is the overall effort of the project. There is no perspective on when, who, what, or how to work. The effort obtained by the bottom-up approach is cumulative; concurrent tasks are not considered, and estimates are calculated from the values obtained from the top-down and bottom-up approaches to calculate the ap-

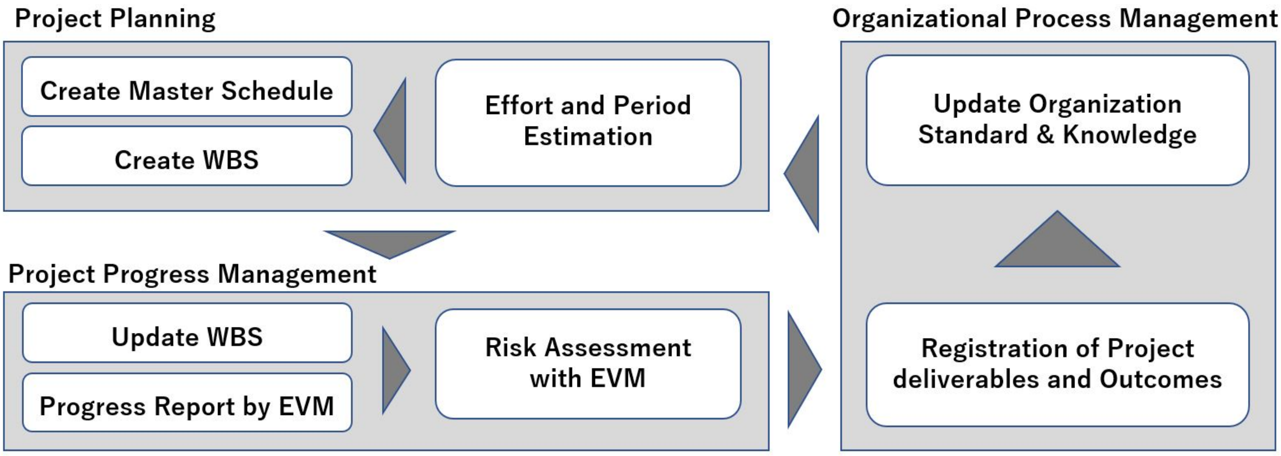

Figure 3: Relationship between project plan, progress management, organization process asset

proximate effort of the project, as presented in Table 1.

3.2.2 Master Schedule Creation

Next, a comprehensive view of the entire project master schedule is created. The master schedule is a sheet of paper that lists all the processes, milestones, and major events from start to finish of the project: Program Evaluation and Review Technique (PERT) projection.

Once the master schedule is completed, the critical path refers to a path that cannot be accelerated owing to the dependency on the processes and tasks. By applying the organization's development phase to the critical path and visualizing the start, inter-process dependency, and minimum lead time, reliable process management becomes possible.

In the master schedule, the development process is described up to the WBS code, with another stage breakdown, and the required time is expressed as the length of the horizontal line of the PERT. In this study, we used the three-point estimation method, which is used in management and information systems applications for construction. In the three-point estimation, three parameters were used based on prior experience or best-guesses :

a = the best - case estimate
m = the most likely estimate
b = the worst - case estimate

These values are calculated as the E value that considers both the most optimistic and most pessimistic estimates provided.

$$E = (a + 4m + b) / 6$$

3.2.3 WBS Creation

Once the master schedule is created, the effort for the entire project and the start and end dates are fixed, and how long it takes for each development period is known. The WBS is created, as shown in Table 2. The left side of Table 2 is "WBS," which is the top-level content consistent with the master schedule. The "WBS Dictionary" on the right side of Table 2 refers to the person in charge, the necessary man-hours, the start date, and the end date, and the specific tasks used for progress management.

It is difficult to detail the WBS at the project planning stage; therefore, the project planning is equivalent to the master schedule. However, when the project starts, each development phase breaks down into manageable tasks. A manageable task is to break down a person's task into no longer than five days, start–end date, and effort.

3.3 Project Progress Management

3.3.1 WBS Update

The project progress management process was conducted in progress meetings held by the project bodies. In many projects, progress meetings are held once a week and the WBS is updated accordingly.

In updating the EVM, the cost accounting standard for activities will be "50%-50% rule." When the work begins, 50% of the estimated man-hours will be recorded as progress. After that, the remaining 50% will be recorded upon completion, not until completion. The EVM's accounting methods include "0%-100% rule," "20%-80% rule," and so on. In this study, simplicity is prioritized over strictness because progress management is held once a week and activities are within five people's days; therefore, even if progress is delayed, most of them are expected to be caught up the following week.

By updating the EVM, the parameters at that time are obtained. Figure 4 shows the EVM concept and the parameters used in progress management. This graph shows the costs along the vertical axis and time on the horizontal axis. In the planned value (PV) of this graph, the proficiency curve (S-curve) is the cost baseline. This is the planned cost of an activity based on the schedule.

The EVM basically understands PV, EV, and AC at the project site, and other values can be calculated; therefore, the other parameters are calculated by the formula built into the WBS form. The results are presented in Table 3.

3.3.2 Progress Report by EVM

In previous progress meetings, there were many subjective and ambiguous reports. This study eliminates this ambiguity

Table 2: WBS and WBS Dictionary

WBS			WBS Dictionary					
Phase Name	WBS Code	Work Package	Author	Estimated Start Date	Estimated End Date	Estimated NOS Items	Average Effort	Estimated Effort
Design Phase	Screen Design	State transition diagram	AAA	MM/DD	MM/DD	10 items	2 Days	20 Days
...	...	...	...	...	...	...	...	...

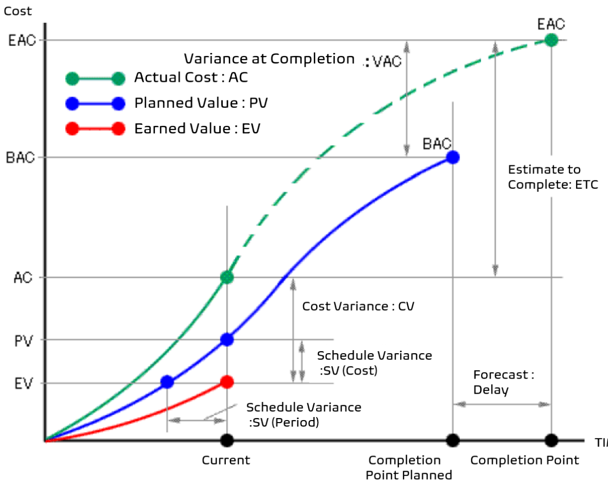

Figure 4: Concept of EVM

Table 3: EVM Terms and Calculation

Abbrev	Translation	Calc
BAC	Budget at Completion	
PV	Planned Value	
EV	Earned Value	
AC	Actual Cost	
SV	Schedule Variance	EV-PV
CV	Cost Variance	EV-AC
SPI	Schedule Per Index	EV/PV
CPI	Cost Per Index	EV/AC
ETC	Estimate to Completion	(BAC-EV)/CPI
EAC	Estimate at Completion	AC+ETC
VAC	Variance at Completion	BAC-EAC

and provides objective reports using EVM values, as shown in Table 4, which describes the progress measure.

This study regards man hours as the cornerstone of project progress management. It predicts future man-hours excesses, always conscious of the cost difference between completion and variance at completion (VAC). The EVM volume is equivalent to the cost. Project progress management uses ”man-day” frequently, so costs can be regarded as ”man-day.” It has been reported that the expression ”SV is -five man-days.”

3.3.3 Risk Assessment with EVM

After receiving the report from each person in charge, we conducted progress analysis and risk assessment using the parameters of the EVM. The standard values for the progress analysis are presented in Table 5.

In the progress analysis, if the SPI or CPI reported exceeds the ”standard value” in Table 5, it is noted as ”smokey.” If the delay continues for more than 3 weeks, or if the delay increases, it will be judged as ”fire-extinguishing” and ”fire-extinguishing team” will be introduced.

In the risk assessment, a time series analysis of SPI and CPI is performed, as described in Fig.5. A graph is created with CPI along the vertical axis and SPI on the horizontal axis, and each delay is visually identified as accelerating or stopping falling. If CPI decreases at the same time as SPI, development productivity (SPIxCPI) will decrease and man-hours will significantly exceed expectations. Alternatively, if you know that you are sacrificing CV to maintain SV from a certain point in time, you can estimate that you are compen-

Table 4: Measure of Progress

ECM Express	Changes
SV is -5 days	Report SV values instead of reports like “one week delay”
ETC is 50 man-days	ETC is reported to understand “So What”
SPI is lower than 0.9	Quantitatively reports the delay, not the “slightly late” report
VAC is 50 man-days	VAC is reported as a quantitative value of delay

Table 5: Measure of Progress

Measure	Criteria	Description
SPI	<0.9	Schedule progress delayed by 10%
CPI	<0.9	Cost Progress delayed by 10%
SPI*CPI	<0.8	Development Productivity delayed by 20%
EAC/BAC	>1.1	10% cost over when completed

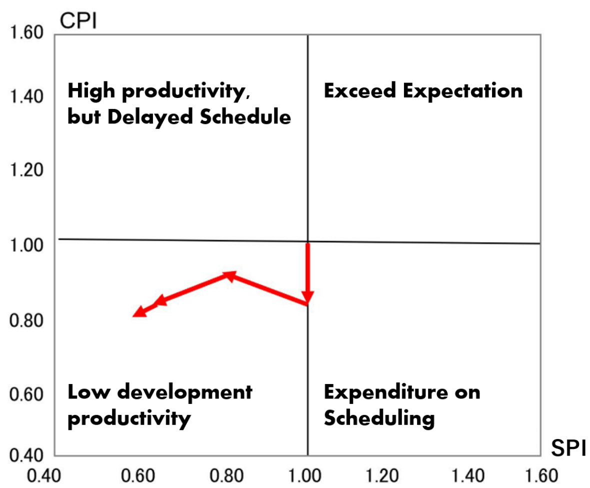

Figure 5: SPI/CPI Time Series Analysis Example

sating for it by working overtime or taking time off if you do not include additional factors.

Finally, we use EAC/BAC to determine the overall status of the project; if the EAC/VAC value exceeds the threshold (e.g., 110%), it means 10% or more of the cost overruns of the plan at the end of the project. These escalate to senior management, who make decisions such as acceptable project cost deficits and push customers for extra staff to ensure quality.

3.4 Organization Process Management

3.4.1 Registration of Project Deliverables and Outcomes

After completing the project, all work products and process assets of the project will be registered in the organizational process asset database.

Generally, the means to increase productivity include increasing the mechanization rate, concurrency, utilization rate, and reuse rate. In the case of manufacturing, such as in system development projects, improvements in reuse will greatly contribute to productivity improvement.

In addition, activities, such as project management, can inevitably lead to trial and error. By reusing the process assets of successful projects, one can expect to save trial and error effort.

Organizations that use CMMI plan the work output for each development phase of the configuration management plan. Keep a record of the work output consistent with this plan. In principle, all the work output of a project should be registered in the organization process asset database and reused in the next project.

3.4.2 Organization Standard and Knowledge Update

In the proposed method, decisions are made in the following parts of the project using intuition and subjective judgments.

- In estimating man-hours, we combine the top-down approach and the bottom-up approach to make estimates. At this time, we do not simply take intermediate values, but make decisions based on the knowledge of experienced people.
- Using the CoBRA method, we use parameters that express the knowledge of experienced people as quantitative values.
- In the PERT projection of the master schedule, pessimistic and optimistic values are calculated using rules of thumb when defining the period of the development phase.
- Progress analysis was conducted using EVM values at the progress meeting, and thresholds for values such as SPI/SPI, VAC/EAC were determined.
- Based on the project period, we use a rule of thumb to determine how long the delay can be recovered.

Once the project is completed, we will verify whether such a subjective judgment is correct and include it in the process asset database as a lesson learned. These lessons are not something that can be used as is, so we aim for a spiral-up by turning this cycle many times.

If you do not have the experience, it is not good to think that you can ask about the experience even if you are in the same organization . Since the rules of personal experience are tacit knowledge, implicit knowledge is likely to be lost owing to retirement or other reasons. You must quickly formalize it and incorporate it into organizational knowledge.

4 APPLICATION RESULT

The results of the application of the proposed method at Company C, which appeared in the case analysis in Section 2, are explained herein.

As explained in Section 2.3, Company C is the company in which the author worked. The author was conducting in-house consultations at Company C for CMMI level acquisition. Until the author joined the company, progress was managed ambiguously. The author proposed the introduction of this method and implemented it over a period of approximately three years.

Company C is developing embedded software for measuring the instruments. Derivatives such as enhancements are

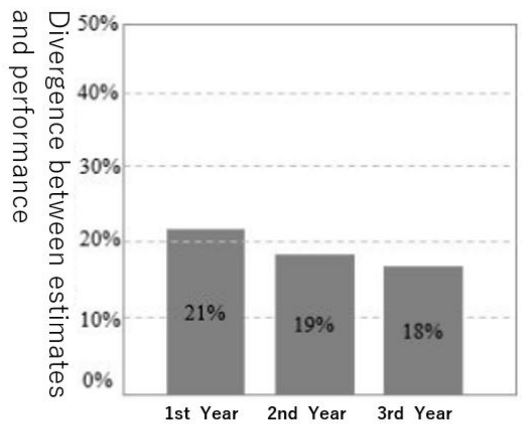

Figure 6: Changes in VAC Ratio to Total Effort

often used in manufacturing measuring instruments. It is difficult to apply the function point (FP) method for the development of embedded systems with precision instruments.

When the company applied this proposal method, SLOC estimated the scale of modification of the previous derivative development of the same model and the area to be modified. Next, considering the frequency of customer demand changes, difficulty of neck technology, and frequency of interface changes, the CoBRA method was used for conversion into man-hours.

Next, we created a WBS for this development by reusing the WBS from the previous derivative development project and estimated man-hours by accumulating the described man-hours. Finally, we calculated the man-hours for this project by combining the two.

After completion of the project, the accuracy of the estimates was measured using the VAC value. The following graph shows the change in the estimation error for approximately three years after the introduction of the proposed method.

In the first year, the difference between the estimates and VAC performance was more than 20%. Three years ago, it had improved by 3%, as shown in Fig.6. This company has adopted only this proposed method, so the improvement effect can be attributed to the proposed method.

5 DISCUSSION

Here, we examine the evaluation of the problem solving described in Section 2.3, and the effects of other process improvements.

5.1 Evaluation of Problem Resolution

5.1.1 Absence of Project Baselines

In this study, as part of project progress management, we proposed a method that takes man-hours as the basis. We created a project plan based on man-hour estimates and managed progress using WBS and EVM.

We solved the problem of vague and unfounded progress reports, such as "one week behind schedule," which was common in previous progress meetings, and made it possible to use objective and quantitative parameters in progress reports.

5.1.2 Feasibility Has Not Been Assessed

In this proposal, experience in the organization's process assets is used for estimating man-hours in the upstream process, determining progress in the development phase, and risk in process management.

For example, in the upstream process, a realistic estimate is made by combining top-down and bottom-up approaches, and after the project is completed, the certainty of the estimate is verified using VAC. In the next project, we will use this learning for estimation.

In our next project, because we are working on the estimation error of the previous project, the estimation error will be more accurate. The rule of thumb is used to avoid repeating the same failure, and it can be evaluated as a feasible methodology.

5.1.3 Lack of Skills Related to WBS

Organizations repeatedly accept projects with the same difficulty and size. Therefore, once WBS is completed and registered as an organization's process assets, the majority can be reused.

In addition, this study established the "50%-50% rule" as the accounting standard for WBS and established the standard value for interpreting the EVM. Consequently, objective risk assessment that was not dependent on the EVM value was also possible.

Organizations that achieve CMMI level 3 rarely have the opportunity to create WBS from scratch and can use historical data. The lack of skills related to WBS was eliminated by standardizing the start of WBS use, EV accounting, and EVM value interpretation.

5.1.4 Lack of Cost Progress Measures

In EVM, whether the cost should be the amount or time is debatable. In this study, we used man-days as the cost of EVM and used it as a consistent progress scale from upstream processes. By using cost as man-days, progress scales such as SPI and CPI can be quantitatively evaluated.

5.2 Impact of Process Improvement

5.2.1 Progress Reports Ambiguity Elimination

In the project subject to this application evaluation, EVM was consistently used in the progress report. Now the report format is "-10 man days for PV" instead of "delayed by about a week."

Company C conducted this basic operation throughout the project period, and there was no confusion when using this method. EVM is supposed to measure the cost in hours or money, but this method is basically the same because the cost is recorded in man-days.

In the previous method of reporting, "delayed by about a week," it was unclear whether that week was a week on the calendar week of work (i.e., a five-person day), but as we were unable to report "one week" after this proposal, it was evident that the delay was a five- or seven-person day.

By implementing the basic action at the progress meetings, the things that no one had noticed, even if they were left ambiguous, were replaced by quantitative expressions. This is also considered an improvement.

5.2.2 How to Grasp the Time of the Progress Meeting

At Company C, the progress meeting was held once a week from 10 a.m. to 12 a.m. on Fridays, and the company worked eight hours a day five days a week; thus, two hours out of 40 hours a week, excluding overtime, were held in progress meetings.

Generally, the time spent on system development is classified into three categories: manufacturing, regular meetings, and management. It is said that approximately 15-20% of the time spent on management is appropriate.

Until the introduction of the proposed method, Company C regarded the time of the progress meeting as a regular meeting, but after the introduction of the proposed method, it was able to grasp the progress of WBS tasks, quantify the progress of the entire project, and calculate future risks.

Whether to have a regular meeting or management time is decided subjectively to some extent when the person in charge records the time, so it is difficult to evaluate the increase or decrease in specific numbers.

However, since the introduction of this proposal method, stakeholders who participated in progress meetings have come to view progress meetings as a place for project progress, so the time taken for regular meetings has decreased, and time for inevitable management has increased.

6 CONCLUSION

This study focused on individual process improvement, such as ”progress management.” The so-called best practices, like CMMI, just include what to do, but do not provide enough description of how to do it.

Therefore, we proposed man-hour-based practices, such as estimating man-hours at the project planning stage, meeting progress at the process management stage, and registering process assets after the project is completed.

By using this method, we eliminate subjective and ambiguous progress reports, such as ”delayed but good,” that were used at previous progress meetings, and are able to quantify the risk assessment using EVMs, so we can see how much cost will be overrun at the end of the project.

However, this study did not evaluate the EVM threshold. For example, the SPI/CPI threshold started at 0.9, because companies such as IBM and Unisys set the threshold at 0.9. However, the pros and cons of small and medium-sized enterprises imitating the practices of large enterprises, such as IBM, have been repeatedly discussed, and if $\text{SPI} < 0.9$, the risk of becoming obsolete is indicated.

It is reasonable to spiral up by accumulating the lessons learned. Establishing correct thresholds for each development site will be a challenge in the future.

REFERENCES

[1] M. Proano-Narvaez, et al, “Earned Value Method (EVM) for Construction Projects: Current Application and Future Projections,” Buildings, Vol. 12, No. 3, 301(2022).

[2] G. Rong, et al, “CMMI Guided Process Improvement for DevOps Projects: An Exploratory Case Study,” 2016 IEEE/ACM International Conference on Software and System Processes (ICSSP), pp. 76-85, (2016).

[3] S. Chunli et al, “Research on Software Project Quality Management Based on CMMI,” 2016 International Conference on Robots and Intelligent System (ICRIS), pp. 381-383, (2016).

[4] M. Choetkiertikul, et al, “A CMMI-Based Automated Risk Assessment Framework,” 2014 21st Asia-Pacific Software Engineering Conference, pp. 63-68, (2014).

[5] C. Rojrattanakorn et al, “Automated Risk Identification of CMMI Project Planning Using Ontology,” 2017 5th Intl Conf on Applied Computing and Information Technology/4th Intl Conf on Computational Science Intelligence and Applied Informatics 2nd Intl Conf on Big Data, Cloud Computing, Data Science (ACIT-CSII-BCD), pp. 19-24, (2017).

[6] A. Odeh, et al, “A Model for Understanding Project Requirements based on CMMI Specifications,” 2021 International Conference on Engineering and Emerging Technologies (ICEET), pp. 1-6, (2021).

[7] Introduction to CoBRA method, CoBRA Laboratories, Ohmsha, (2011).

[8] Y. Mizukami, et al, “Improvement of Workload Estimates by using project characteristic based on CoBRA Method for Software Development Project,” Journal of Japan Society of Directories, Vol 11, pp. 36-45, (2013).

(Received: September 24, 2021)
(Accepted: August 23, 2022)

Akihiro Hayashi received his MBA and Ph.D. from the University of Tsukuba, Tokyo, Japan in 1997 and 2010, and his Ph.D. in Software Engineering from Nanzan University, Nagoya, Japan in 2019. His professional career includes global companies such as Motorola USA, NTT, and IBM Japan. In 2018 he has become a Professor of Department of Information Design, Faculty of Informatics, Shizuoka Institute of Science and Technology. His current research interests include process improvement, quantitative project management, operating research and management strategy. He is a member of IEICE and INFSOC.

Industry Paper

LoRa Communication Method for Growth Management using Image Data

Mikiko Sode Tanaka*, Hikaru Yabe**, and Koichi Tanaka***

* International College of Technology, Japan
** Kanazawa Institute of Technology, Japan
*** Mitsubishi Electric Corporation, Japan
sode@neptune.kanazawa-it.ac.jp

Abstract - "Nototemari" which is a kind of mushroom, is a representative agricultural product of Ishikawa Prefecture. It is cultivated in a greenhouse in Noto's Satoyama. In this paper, we report the results of a study on the construction of a remote monitoring system for Nototemari cultivation. The Nototemari cultivation greenhouse is far away from the management office, so it is costly to visit the greenhouse to monitor the growth. In addition, many producers are elderly. Therefore, we thought that we could improve the efficiency of cultivation work at low cost by constructing a private 115 LoRa network and periodically sending image data of the growth status to the management office. However, due to the slow transmission speed of LoRa communication, it took a long time to send the image data as it was. Therefore, we have built a mechanism to transmit image data in a practical time by recognizing important monitoring points using the object detection based on deep learning, not degrading the image quality of that part, and transmitting the other image parts with degrading or trimming the image quality. In this paper, we show the image data compression method, and the experimental results of the communication method. We will explain the effect of the proposed method.

Keywords: LPWA, LoRa, Production control, Agriculture, Image data

1 INTRODUCTION

In Ishikawa Prefecture, producers, agricultural organizations, markets, prefectures, etc. have come together to brand the grown shiitake mushrooms as Nototemari, which is suitable for the climate of Noto's Satoyama, and is located in the OkuNoto area. However, since the Noto's Satoyama, especially the greenhouse that grows Nototemari, is located in the mountains of Noto, it is a blank area of radio waves and almost no communication environment [1]. In addition, it is difficult to get the power supply. Therefore, it is difficult to use a remote monitoring system that uses cameras and sensors, and all cultivation is carried out manually. Many producers are elderly, and it is desired to reduce the man-hours for patrols.

In recent years, the use of LPWA, which does not require communication charges, has been progressing. No license and application is required as it uses a license-free frequency band. In particular, the private LoRa allows us to install the base station ourself, enabling flexible system design. In addition, 250mW LoRa has a long transmission distance and is often used in mountains [2]. As shown in Fig. 1, we thought about build a private LoRa wireless communication network in Noto's Satoyama, to manage the growth of Nototemari. The problem is that it has a narrow bandwidth and very little data can be sent. It is possible to send sensor data such as temperature and humidity in a short time, but it is very difficult to send image data and video data. Therefore, research is being conducted to send image data with LoRa [3 - 6].

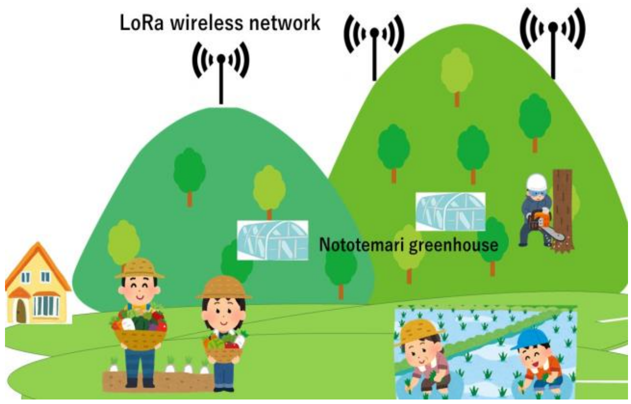

Figure 1: Wireless communication environment aimed to build in Noto's Satoyama

In LoRa technology, total transmission time is limited from the viewpoint of the occupancy prevention and affects to the entire transmission time for large data like image data. Therefore, it is said that it is difficult to send image data and video data. In addtion, generally, LoRa platform assumed to be inappropriate to transmit high bit rate data, such as image data or voice data, due to its narrow bandwidth accessible for physical layer modulation. Bandwidth (BW) and spread rate (SF) can be changed with LoRa technology. The narrower the bandwidth and the higher the diffusion rate, we can detect the signal farther. However, the narrower the BW and the larger the SF, the longer the transmission time and the higher the power consumption. In other words, it takes time to transmit data to fly far.

The first attempt to transfer image data over a LoRa network was presented in [4] by C. Pham in 2016, a year after the introduction of the LoRa framework. C. Pham proposed a low cost and power visual supervision platform based on image data compression and a change detection technique. The image data compression implemented a packet loss-tolerant image compression technique that can run on very limited memory platforms. The results from the tests showed that an image data of about 2.4 KBytes could be transmitted up to 1.8 km. Although in this work, it is difficult to be used for external surroundings with continuously variation of brightness.

Chen et. al. [5] proposed a light trustworthy communication protocol called MPLR for image data transmission in LoRa. It facilitates image monitoring in an agricultural IoT platform. The MPLR protocol groups information packet transmissions. By returning one ACK for each group, the time required for ACK is reduced. The test results showed that MPLR protocol during the image data transmission procedure decrease the time by 24%. This method is effective when there are few data transmission errors. Therefore, it is not suitable for large size data.

Ji et al [6], proposed a method in which doesn't transmit full images in order to reduced data rate and bandwidth. Full images are not needed to be transmitted, and by this way bandwidth usage on LoRa can be reduced. The scheme took advantage of the static feature of various areas and especially in farming by suggesting a new monitoring plan that splits every image into tiny grid patches. But this method observed that most points in an image must be static, and significant changes are not allowed.

In order to solve the problem of the conventional method, we propose a new method to divide the photo into the part that the producers want to see and the part that is not so important, and transfer the not important part with reduced image accuracy. The proposal system uses the object detection with deep learning to discover important points. This makes it possible to increase the rate of image data compression. By reducing the image data size, the load and time required for transmission can be reduced, and a practical system can be constructed.

LoRa is expected to be used in various systems because it is license-free and does not require communication costs. However, it has been unsuitable because the amount of data that can be transmitted is small and it takes time to transmit images. We propose a method to reduce the transmission time by extracting and transmitting only the necessary portion of the image. In this paper, we explain the image data compression method and the communication infrastructure using a private LoRa that is the basis of the remote monitoring system. Also, we explain a protocol and a frame data set for the system. In addition, we explain the result of the conduct a demonstration experiment.

2 SYSTEM COMFIGURATION

2.1 Remote Monitoring System

LoRa is a communication standard using spread-spectrum modulation techniques developed by Semtech Corporation. 20mW LoRa is widely used in Japan because it can be used in specified low power radio stations that do not require a license. In recent years, efforts have begun to utilize 250mW LoRa in the disaster prevention systems and the bus location systems [7 - 8]. It is also being used in mountainous areas by taking advantage of long-distance transmission [9]. There is a report that 160km transmission is possible in mountainous areas [9]. 250mW LoRa is more difficult to use than 20mW LoRa because it requires a registration license, but considering its transmittable distance, it is effective as a means to solve the situation where there is no communication environment in the mountains. We decided to use 250mW LoRa.

The system configuration of the remote monitoring system for Nototemari will be described. Since mobile phone networks are often unavailable, it is assumed that in the greenhouse, in addition to temperature and humidity, a photo will be taken once a day and sent from a private LoRa to the management office. Due to the distance between the greenhouse and the management office, there are several repeaters in the proposed configuration where the data is sent to the management office via the repeaters. The 250mW LoRa has a long transmission distance even in the line of sight, but there are undulations in the mountainous areas, and there are parts where the transmission distance is short depending on the location. Therefore, repeaters are indispensable. Figure 2 shows the overall image of the remote monitoring system for Nototemari.

Since the management office is located in Satoyama, only telephone lines can be used in many cases, so the system configuration allows data to be uploaded to the cloud using telephone lines. Greenhouses often do not have a power source, so it may be necessary to obtain electricity from solar power. Therefore, the power is turned off except for acquiring data once a day and transmitting it.

The repeater holds two LoRa modules. One is for reception and the other is for transmission. When the receiving LoRa receives a packet, the packet data is registered in the buffer folder. This process is repeated until all the data is received. The sending LoRa checks if there is data in the buffer folder, and if there is data, sends it in the order of the oldest generation time. Also, it will check if there is data on a regular basis. With these two LoRa modules, data can be sent to the next node without stagnation. Depending on the distance between the management office and the greenhouse, multiple repeaters may be placed.

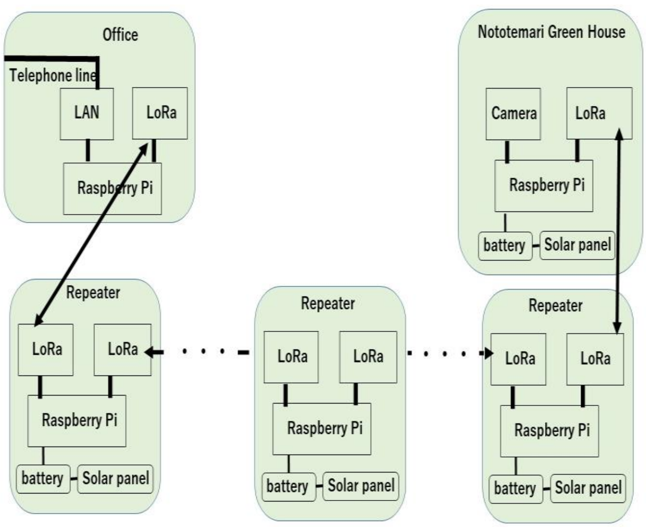

Figure 2: System configuration of remote monitoring system for "Nototemari"

Temperature and humidity are important factors for the growth of Nototemari [10]. Humidity is especially important. In addition, there are many items that should be visually confirmed, such as how the umbrella is wrapped, and images are important for growth management [10 - 11]. For these reasons, a temperature / humidity sensor and cameras were installed in the greenhouse, and these data was transmitted to the management office using a private LoRa network so that it could be confirmed at the management office. Since LoRa has a narrow band, it is difficult to send image data as it is. Therefore, we needed to reduce the size of the data. We decided to use the object detection based on deep learning to extract only the necessary parts and send them.

2.2 Image Data Compression Method

Data compression is important for transferring data within the time limit. In order to compress the data, it is common to reduce the resolution of the data. However, this method is not suitable for careful observation of growth. Therefore, we decided to extract and send only the important parts. We succeeded in compressing the amount of data while maintaining the image quality required for growth management. Figure 3 shows an example of image data compression. The left is the data before compression, and the right is the data after compression. In this example, unnecessary parts are filled with white. If it is better to understand the appearance of the log from the outline alone, reduce the resolution of the unnecessary part or extract the outline to make only the outline. The compression level can be specified. The items that should be observed carefully are first learned, and the learning results are used for recognition. Items that perform object detection can also be controlled. It's important to be able to control, as each growth process has different items to check.

Figure 4 shows the processing flow for acquiring image data and sending it with a private LoRa. First, a picture is taken. Second, the object detection with deep learning is performed. In order to recognize the important part, acquire the training image data in advance, train these, and create a library. This library is used to recognize important parts, maintain the image quality of those parts, and compress the image data size by transmitting the other parts with reduced image quality. Next, the image data is changed to the video data, and the video data is performed compression in H.265 [12], it transmits and receive data at a private LoRa.

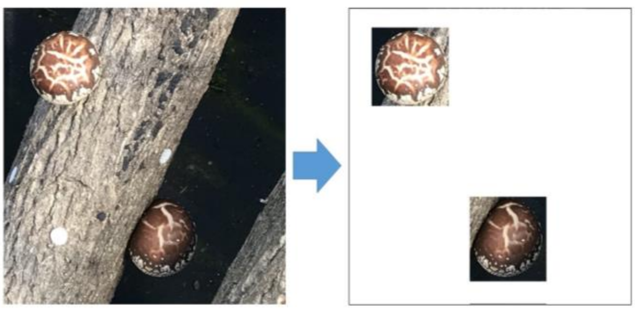

Figure 3: An example of image data compression
(Left: before compression, Right: after compression)

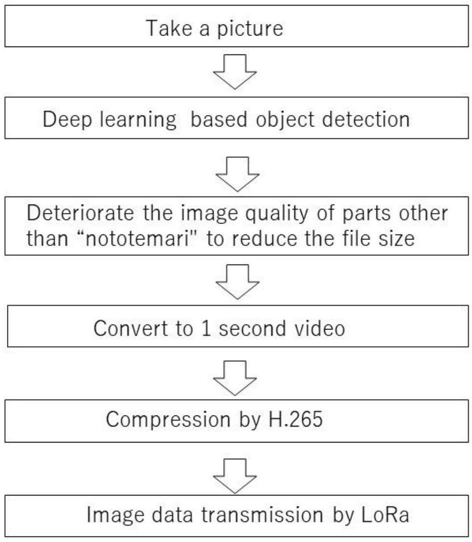

Figure 4: Greenhouse side system flow of remote monitoring system for Nototemari

H.265 is a video compression standard and can achieve equivalent image quality at half the file size and bit rate of H.264. Therefore, the file size has been reduced by converting H.264 files to H.265. H.265 optimizes the block according to the amount of change. In H.265, a block with few changes and a simple block change to a large block, and a block with complex changes change to a small block. This reduces the total amount of information. The larger the block size can be made, the fewer the number of blocks. As a result, the file size can be reduced.

H.265 is a video standard, but it also define about still images as a subset. However, there are restrictions on still images, such as restrictions on the supported bit depth [13]. In order to use the H.265 standard effectively, it is desirable to use as video. Therefore we decided to change the still image to a video. A 1 second video was used because 1 second was easy to handle due to the system construction.

Image compression is performed by lowering the image resolution or filtered for feature extraction except for the part that farmers want to focus on. In extreme cases, the areas that are not in focus are painted white. The data size by filling the unnecessary parts with white is reduce, and by keeping the position of the Nototemari, it is possible to imagine the whole. If the image data size is large, it will take time to send. In addition, the possibility of transmission errors increases, which is not desirable for the system. Therefore, we decided to send the high accuracy only the parts that the producer must confirm with high accuracy. This makes it possible to send in a few minutes, which is practical.

3 COMMUNICATION PROTOCOL AND FRAME STRCTURE

3.1 Frame Structure

Multiple frames such as an image data transmission frame and an environment data transmission frame are prepared to be able to extend to monitoring functions of agricultural workers such as emergency communication. Here, the image data transmission frame and the environment data transmission frame will be described.

Figure 5 (a) shows an image data transmission frame structure. With LoRa, a maximum of 255 Bytes can be transmitted with one transmission. The first 24 Bytes is the module-specific usage area we are using. Next, the payload comes, and the image data is put in this area and transmitted. As shown in Fig. 6, the image data is divided into 225 Bytes and transmitted, and the receiving side connects the received data into one file. The first Byte of the payload is the data number. The next divided image data 225 Bytes is stored. The next 1 Byte is the control code. In the case of image data, “Null” indicates that the data has a continuation. “\ n” indicates the end of the data. This 1 Byte indicates what purpose the frame is used for. In the case of image data, the data is transmitted using multiple frames, but in the case of environment transmission data, it is completed in the one frame. The last 3 Bytes are space for the module.

Figure 5 (b) shows an environments data transmission frame structure. The first 24 Bytes is the module-specific usage area we are using. Next, the payload comes, and the environment data is put in this area and transmitted. We can put a control code in the next 1 Byte. The character code written in the control code determines what data is contained. The last area is the area where the LoRa module we are using is used.

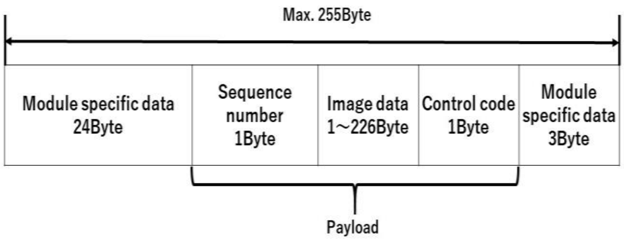

(a) Image data transmission frame structure

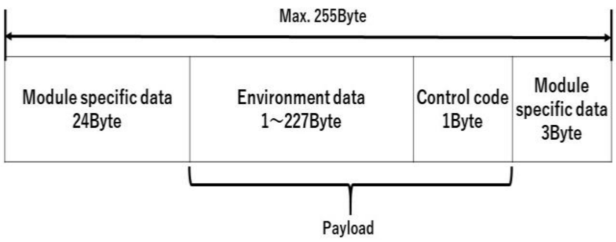

(b) Environments data transmission frame structure

Figure 5: Frame Structure

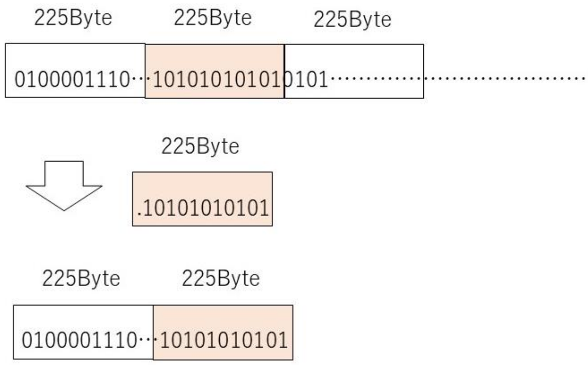

Figure 6: Image data transfer image

3.2 Communication Protocol

The communication protocol is the stop-and-wait scheme [5]. That is, after sending the data, change to the receive mode and receive an ACK indicating that the data has been received. If the ACK is not received even after waiting for 15 seconds, the data will be sent again. This process is repeated until an ACK is received. Since temperature and humidity send one piece of data in one frame, data is sent using this protocol.

The communication protocol for image data transmission is shown in Fig. 7. The communication protocol used in the image data transmission is also the stop-and-wait scheme. The procedure will be explained. The first 225 Bytes of untransmitted data are taken out and sent from the LoRa device in the greenhouse to the Gateway. When the Gateway receives the data, it returns an ACK indicating that it has received it. This process is continued until all the data has been transmitted. If the transmission fails and the ACK cannot be received, resend will wait 15 seconds and the data will be retransmitted.

The problem in implementing the stop-and-wait scheme is that it cannot determine the duplication of packets. If an Ack sent from the receiving side to the sending side is lost or corrupted, the sending side times out and retransmits the frame. In this case, the receiving side will have two frames with the same content, and the data will not be consistent. To solve this problem, a sequence number is defined in the first Byte of the frame, and 0 and 1 are entered alternately for each transmission. This allows the receiving side to detect duplicate frames by checking if the sequence number is entered alternately.

When there is no more data to send, the sender sends an exit character. The receiver receive the exit character, completes the reception and sends an Ack to the sender. This completes the sending and receiving process. After that, the receiver continues to wait for data to be received.

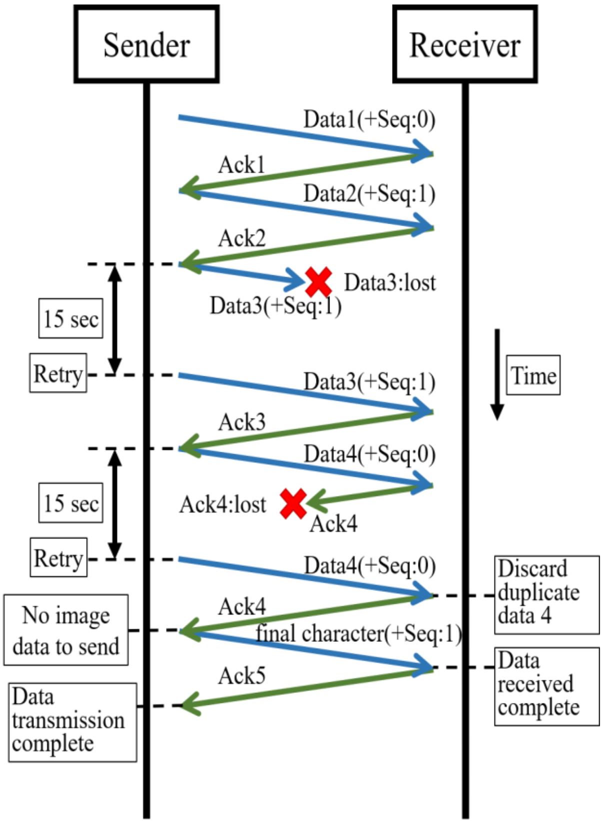

Figure 7: Communication Protocol

4 EXPERIMENTAL RESULTS

In this chapter, we will evaluate the proposed image data compression method to enable transmission and reception of images using LoRa. In addition, the result of visual verification that there is no problem in the image accuracy for the observation target even if the image data compression is performed is shown. In addition, it shows that the compressed image data can be transmitted using LoRa in a reasonable time. Figure 8 shows an example of a camera installed in the Nototemari greenhouse. In this experiment, four cameras were installed in one greenhouse at different heights and locations. Since the camera is installed in the frame of the greenhouse, it is difficult to shoot from a short distance.

4.1 Object Detection Experiment

We will explain the experiment of image data degeneracy using the object detection based on deep learning. We collect photos of what we want to check in advance and we let learn. The work of collecting photos was done with the cooperation of the Ishikawa Agricultural Experiment Station. Yolov5 was used for the learning and the object detection [14].

Learning of yolov5 is very time consuming. However, once we can make a library, we can continue to use it. Therefore we make it in advance. The learning process was done on a homebrew PC (CPU is Intel CPU BX8070110900K Core i9-10900K processor 3.7GHz 20MB

Figure 8: Camera installed in the Nototemari greenhouse

Figure 9: An example of image data which is extracted object detection

cache 10 cores. The graphics board is the MSI GeForce RTX 3070 VENTUS 2X OC graphics board VD7419.). We spent several days for learning. When the training was completed, the trained library is installed in the Raspberry Pi 3b of the sender device.

The object detection was performed on the Raspberry Pi 3b using the trained library. Figure 9 is an example of the result of object detection by yolov5. Nine Nototemaris were detected. This data was used to reduce the image quality of the parts other than Nototemari. The program of the image quality reduction used OpenCV library [15]. In this experiment, other area of not interest were painted white. Table 1 shows the difference in data size. We confirmed the data is reduced to about 1/10. We can see that deleting unnecessary parts helps to reduce the image data size.

Table 1: Comparison of data size between original image data and extracted data

	Data size
Original image data	4,164,000 Bytes
Extracted data by object detection	352,907 Bytes

4.2 Image Data Compression Experiment

We will explain the experiment of image data size reduction to H.265 using ffmpeg [16]. The result of degeneracy using the object detection based on deep learning is shown for the photograph taken at Nototemari greenhouse. Figure 10 is after reduction by the object detection based on deep learning and reduction of the image quality of the parts other than Nototemari. In this example, the part other than the part recognized by the object detection based on deep learning is painted white. Figure 11 shows the reduction results of the file size reduction using H.265. As can be seen from the Fig. 10 and Fig. 11, compression does not have a significant im

Table 2 shows the data size of after conversion to H.265. When compressed with H.265, the data size was 1/5 of that before compression. Table 3 shows the conversion time to H.265. The experiment was done with a Raspberry Pi 3b. The processing time is about 31 seconds and about 21 seconds, which is practical.

Compression using the object detection based on deep learning is different from the conventional method of reducing the image quality of the entire image, and it is possible to acquire high-quality data for the part we want to see. In addition, our system can support for the rotation of logs of Nototemari by producers. That is, there is no problem even if the position of the Nototemari changes in the camera image. Also, if we register a disease etc. in the object detection library, the data will be sent with a clear image of that part, so we will not overlook it.

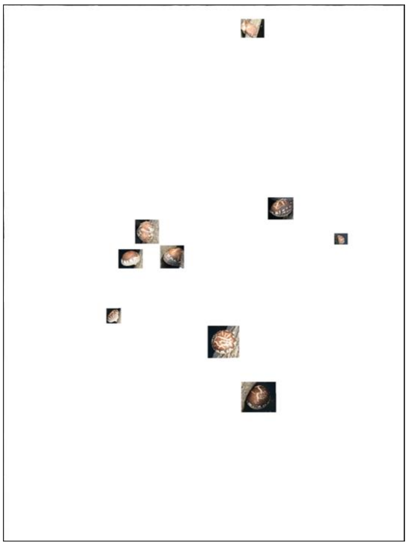

Figure 10: An example of extraction by object detection

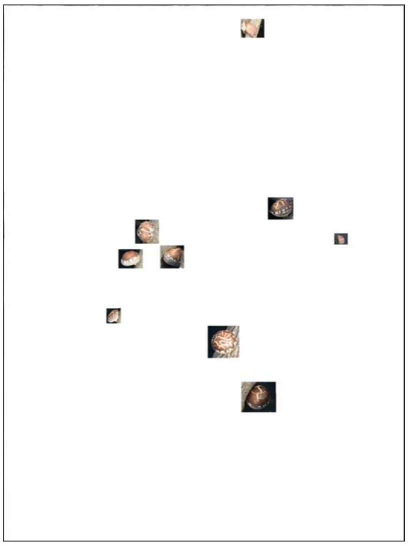

Figure 11: An example of after compression with H.265

Table 2: Data size after reduction

	Data size
Extraction data by object detection	352,907 Bytes
After compression with H.265	69,955 Bytes

Table 3: Processing time of image data compression

	Processing Time(s)
Extraction by object detection	31.477
Compression with H.265	21.338

H.265 also has the disadvantage of enormous calculation costs for encoding time. In fact, the compression process to H.265 took about 21 seconds on a Raspberry Pi 3b. However, considering the transmission time in LoRa, we thought that data should be compressed by an edge computing even if it takes time.

4.3 Data Transmission Experiment

In this chapter, we explain the LoRa transmission test experiment. We tested how long it takes to transmit a compressed image data. Figure 12 shows the experimental environment. The experiment was conducted indoors. The experiment was done with a Raspberry Pi 3b. This is a communication experiment between gateway and a sender unit. A sender unit takes a picture, detects an object, compresses data, and transmits with LoRa. In this experiment, the image data to be transmitted was prepared in advance, and only the image data transmission was tested.

Under the restriction of a law in Japan, when LoRa communication is used, the time that can be continuously transmitted is set to 4 seconds. Therefore, the size of data that can be transmitted at a time varies depending on parameters such as SF and BW. In order to improve the efficiency of communication, we need to change the size of data that can be sent at a time depending on the SF and BW. Table 4 shows the correspondence between the parameters and the communication speed. SF9, BW 125MHz can send data to the farthest distance, but the amount of data that can be sent is the least.

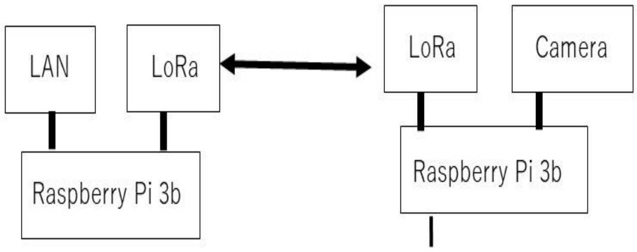

Figure 12: LoRa transmission test environment

Table 4: Correspondence table between parameters and communication speed (bps) [17]

	BW 125 kHz	BW 250 kHz	BW 500 kHz
SF7	5469	10938	21875
SF8	3125	6250	12500
SF9	1758	3514	7031

Table 5: Transmission of extracted data by object detection

		BW 125 kHz	BW 250 kHz	BW 500 kHz
SF7	Send time	39m 20s	22m 31s	17m 31s
	Resend count	27	3	4
SF8	Send time	47m 53s	29m 41s	20m 36s
	Resend count	0	1	1
SF9	Send time	1h 28m 14s	43m 12s	32m 15s
	Resend count	51	0	20

Table 6: Transmission of image data compressed with H.265

		BW 125 kHz	BW 250 kHz	BW 500 kHz
SF7	Send time	6m 57s	4m 34s	3m 16s
	Resend count	2	1	0
SF8	Send time	9m 45s	6m 5s	4m 2s
	Resend count	1	1	0
SF9	Send time	18m 28s	8m 49s	6m 39s
	Resend count	14	1	5

We conducted a communication experiment using the image in Fig. 10 and the image in Fig. 11. The results of that experiment are shown in Table 5 and Table 6.

Table 5 shows the results when the image data shown in Figure 10 is transmitted using LoRa. SF has changed SF7, SF8, and SF9. BW was changed to 125 kHz, 250 kHz, and 500 kHz. With SF7 and BW125 kHz, the transmission time is the longest and the number of retransmissions is also large. The larger the BW, the shorter the time to transfer the data. If we change from SF7 to SF8 or SF9, the transmission time will be slower. If the transmission time is long, the number of retransmissions tends to increase. It takes tens of minutes to transfer the data, which is not practical.

Table 6 shows the results when the image data shown in Fig. 11 is transmitted using LoRa. SF has changed SF7, SF8, and SF9. BW was changed to 125 kHz, 250 kHz, and 500 kHz. With SF7 and BW125 kHz, the transmission time is the longest and the number of retransmissions is also large. The larger the BW, the shorter the time to transfer the data. If we change from SF7 to SF8 or SF9, the transmission time will be slower. If the transmission time is long, the number of retransmissions tends to increase. In the case of SF7 and BW 500 kHz, it takes only few minutes to transfer the data, which is practical.

When compressed with H.265, the data size will be about 1/5. We can see that the transmission speed is also about one-fifth. That is, it can be said that using H.265 is effective in reducing the LoRa transmission time and the number of retransmissions. As can be seen from Table 5, it takes a lot of time without data compression. Especially with SF9, some parameters took more than an hour. In contrast, the compressed image data can be transmitted and received in less time even in SF9. The fact that they can be transmitted and received in less time in SF9 leads to a reduction in the number of repeaters installed, thus we can realize a sustainable system.

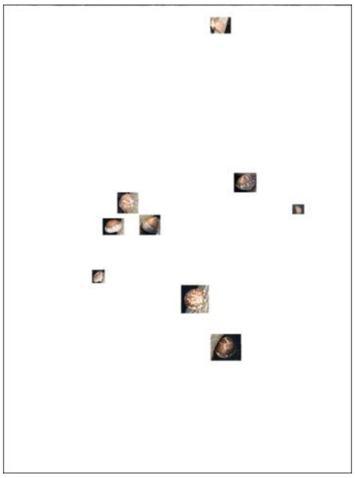

Figure 13: Received image data

Figure 13 is an image acquired by the gateway. We can see that there is no image deterioration of the Nototemari parts compared to the transmitted data. In addition, since the parts that users want to observe with the image quality taken by the camera are retained, it can be said that it is sufficiently practical for growth management of Nototemari. About 4 cameras will be installed in the greenhouse, but if the time required to transfer the data of one image is about 10 minutes, even if all the data is sent, it will be within 1 hour. Thus the system can send the data once a day. Then, it can withstand the operation with the solar panel and battery. It is of great significance for agricultural workers to be able to see the state of the Nototemari in a greenhouse in the Noto's Satoyama at home or in the workplace with clear images. Picture quality was adequate for them in experiment. This eliminates the need to check the status on a regular basis and makes it possible to reduce management costs.

5 CONCLUSION

Nototemari is a representative agricultural product of Ishikawa Prefecture. It is cultivated in a greenhouse in Noto's Satoyama. Noto's Satoyama communication environment is not good. In this paper, we reported the results of a study on the construction of a remote monitoring system for Nototemari cultivation. The Nototemari cultivation greenhouse is far away from the management office where the cultivation is managed, so it is costly to visit the greenhouse to monitor the growth. In addition, many producers are elderly. Therefore, we thought that we could improve the efficiency of cultivation work at low cost by constructing a LoRa network and periodically sending image data of the growth status to the management office. However, due to the slow transmission speed of LoRa communication, it took a long time to send the image data as it was. Therefore, we have built a mechanism to transmit image data in a practical time by recognizing a Nototemari using the object detection based on deep learning, not degrading the image quality of that part, and transmitting the image with degrading the image quality of other parts. In this paper, we show the experimental results of the propose image data sending system, and show its effectiveness. The proposed an image data sending system turned out to be sufficiently practical because one image data can be sent in a short time.

ACKNOWLEDGMENTS

The research is supported by the Telecommunication Advancement Foundation.

REFERENCES

[1] Adhere to radio wave countermeasures on the Noto Peninsula! What is a device that suits the mountains, sea, sightseeing spots, and the natural environment, https://time-space.kddi.com/au-kddi/20200305/2854, Access 2021.5.7.

[2] J.Moribe, A.Fujimoto and Y.Tokita, "Development of a data notification system using GEO-WAVE," IEICE Communications Express, Vol.8, No.12, 536–541.

[3] A.Staikopoulos, V.Kanakaris, G.A.Papakostas, "Image Transmission via LoRa Networks – A Survey,"2020 IEEE 5th International Conference on Image, Vision and Computing (ICIVC), Beijing, China.

[4] C. Pham, "Low-cost, low-power and long-range image sensor for visual surveillance," AMC SmartObject '16, pp. 35-40, (2016).

[5] T.Chen, D. Eager and D.Makaroff, 2019, July. "Efficient Image Transmission Using LoRa Technology In Agricultural Monitoring IoT Systems," In 2019 International Conference on Internet of Things (iThings) and IEEE Green Computing and Communications (GreenCom) and IEEE Cyber, Physical and Social Computing (CPSCom) and IEEE Smart Data (SmartData) (pp. 937-944). IEEE.

[6] M.Ji, J.Yoon, J.Choo, M.Jang and A.Smith, 2019, March. "LoRa-based Visual Monitoring Scheme for Agriculture IoT," In 2019 IEEE Sensors Applications Symposium (SAS) (pp. 1-6). IEEE.

[7] S.Ishikawa, H.Yabe, R.Sakauchi, M.S.Tanaka, "Examination of system configuration considering propagation characteristic difference due to LoRa output power difference - On the Nonoichi community bus route-," IEICE-SR2020-42, (2020/11/11).

[8] T.Moritama, M.Uesugi, "Regional Disaster Prevention Plan with IoT Sensor Network on the River basin and Gaming - For Disaster Prevention Go! -," IEICE-ICTSSL2019-30, (2019-10-10).

[9] J.Moribe, A.Fujimoto, Y.Tokita, "Development of a data notification system using GEO-WAVE," IEICE Communications Express, Vol.8, No.12, 536–541, (2019).

[10] T. Yashirna, J.Kodani, M.Kado, "Influence of different cultivation environment in vinyl house to fruit body development of the large shi i take mushroom," https://agriknowledge.affrc.go.jp/RN/2010922309.pdf.

[11]Nototemari cultivation guide, https://www.pref.ishikawa.lg.jp/ringyo/publish/documents/nototemari2018.pdf, access 2021.5.7.

[12] S.Okubo, T.Suzuki, S.Takamura, T.Chujoh, “H.265 / HEVC textbook,” Impress Corporation, ISBN978-4-8443-3468-2.
[13] G.J.Sullivan, J.R.Ohm, W.J.Han, and T.Wiegand, “Overview of the High Efficiency Video Coding (HEVC) Standard,” IEEE Transactions on Circuits and Systems for Video Technology, Vol. 22, No. 12, Dec. (2012).
[14] Yolov5, https://github.com/ultralytics/yolov5.
[15] OpenCV, http://github.com/opencv/opencv.
[16] http://ffmpeg.org/, access 2021.7.24.
[17]http://www.rflink.co.jp/pdf/RM-92A-92C/LoRa-Communication%20speed%20setting%20table_v2.pdf access 2022.6.5.

(Received: November 16, 2021)
(Accepted: August 8, 2022)

Mikiko Sode Tanaka received Dr. Eng. degrees from Waseda University in Fundamental Science and Engineering. She joined NEC Corporation, NEC Electronics Corporation, and Renesas Electronics Corporation. She is Associate Professor of International College of Technology, Kanazawa. Her research interests include wireless communications, AI chip, and personal authentication. She is a member of IEICE (Institute of Electronics, Information and Communication Engineers). Also, she is senior member of IPSJ (Information Processing Society of Japan) and IEEE (Institute of Electrical and Electronics Engineers).

Hikaru Yabe graduated in March 2022 from the Department of Information Technology, Faculty of Engineering, Kanazawa Institute of Technology, and joined Softbank Corp in April 2022.

Koichi Tanaka received Dr. Eng. degrees from Shizuoka University. He works for Mitsubishi Electric Corp. His research interests include mobile computing, distributed systems and telecommunication protocols such as field servers for cultivations, car navigation systems, and mobile phones. He is a member of IPSJ (Information Processing Society of Japan).

Industry Paper

Low Cost Based IoT System in the Paddy Field to Labor-Saving and Feasible Study for Protecting Japanese Rice Terraces

Kazuma Nishigaki[*], Naohiro Kamatani[**], and Kanae Matsui[***]

[*]Graduate School of Informatics, Tokyo Denki University, Japan
[**]School of Information System Engineering, Tokyo Denki University, Japan
[***]School of System Design and Technology, Tokyo Denki University, Japan
{20jkm23@ms, 21amj05@ms, matsui@mail}.dendai.ac.jp

Abstract - Rice terraces, which are one of the factors that form the traditional landscape of Japan, exist in hilly and mountainous areas. Due to their topographical features and the aging agricultural workers, it is difficult to continue rice cultivation for a long time. Therefore, we focused on water management, which occupies approximately 30% of the working time in rice cultivation and proposed a paddy field water level monitoring system aimed at labor savings using Sigfox communication. We implemented a system that can be used by elderly farmers and conducted an experiment in Otari Village, Nagano Prefecture, to verify the functionality of the proposed system. As a result, we received results from both the quantitative and qualitative evaluations.

Keywords: IoT application, Agriculture, Paddy field, Sigfox, Labor saving.

1 INTRODUCTION

In the field of agricultural IoT, technological innovations in networks, hardware, and software have been progressing. In addition, studies and practical applications have been promoted to develop labor-saving and automation technologies. In this field, the amount of investment and the technological requirements differ greatly between full-time farmers and side business farmers. In addition, since the applicable technology differs depending on the breeding environment, a system that meets the requirements of the agricultural systems is required.

This study focused on labor-saving in water management for part-time farmers in terraced rice fields. Rice terraces are not only valuable as a landscape of Japanese “satoyama”, but are also an important resource in the region because they play a role in disaster prevention by taking irrigated land. However, they are difficult to pave and are not flat. For these reasons, the rice terraces have shrunk, and such a phenomenon occurs in mountainous areas with rice terraces. Therefore, we propose an IoT-based water level monitoring system that can be used by elderly farmers at a low cost for saving labor in rice terraces. Water management accounts for 30% of the agricultural work during rice cultivation, and we aimed to relieve the burden by saving labor. In addition, the proposed system was installed in three farms: the Otari Village, the Kita-azumi District, and the Nagano Prefecture, which are in a mountainous area with terraced rice fields. The usefulness of the system was verified by a quantitative and qualitative evaluation.

The novelties of this paper are (1) the design of supporting paddy field labors and implemented them in a real field as PoC (Proof of concept), (2) revealed the proposed system is reassuring to be able to make decisions on patrols in rainy weather and confirm information from a distance. Later points were important, especially for elderly people who are the main laborers in agricultural fields.

2 RELATED WORK

This section describes water management systems and applications for rice cultivation in the field of agricultural IoT. Before starting the introduction of real products, we describe the IoT-based prototypes for supporting agriculture especially for supporting paddy fields. In the paddy fields, water management is important and there are two types of technologies sense water levels. Former is a sensor to sense water level directly, the other is to utilize image data and analyzed them for sensing water level. Reference [2 and 3] shows IoT sensors can be utilized for sensing water level with inkjet-printed soil moisture and leaf wetness sensor and there are examples of former technologies. The other is showed in reference [4 and 5] and they used the massive image data and machine learning to measure water level in the paddy field.

Our proposed system adopted the former technologies; sensing water level with sensor and networked it for data utilization. Following products shows how IoT-based technologies are utilized for the paddy field management.

2.1 PaddyWatch

This product is a system that automatically measured the water level and temperature required for paddy rice cultivation, which also had a water level sensor in paddy fields sold by Vegitalia Co., Ltd. [6]. This product aims to reduce the number of water patrols and the time required for farmer patrols by providing the water level status on a web application. In addition, it had the necessary functions for proper water management and additional functions for data analysis. The network uses NTT DoCoMo’ SIM. The sensor unit could measure the water level and the water temperature, while optionally acquiring other data. The three series, PaddyWatch, PW-2300, and PW-2400, as of November 10, 2020, have a standard monthly basic charge (use period only) of 1,980 yen.

2.2 Paditch Gate 02+

This product realized real-time remote control of sluice gate management as one of the water management practices provided by Enowa Co., Ltd. [7]. The product has a water level adjustment function, and users could select a time in advance to close a water gate for the paddy fields. Additionally, the product could open and close the floodgate automatically. The sensor unit measures the water level and temperature of the paddy field. In water management, determination, and actions, such as opening the floodgate based on data about water level and temperature could add new water to the paddy field to raise the water level. Hence, if the system sensed that the water temperature would have been lower, the floodgate would have been closed. This product saves labor in water management by remotely controlling and automating the system.

2.3 Position of This Research

The above products for water management in rice cultivation have been expanded and introduced to actual sites. In particular, PaddyWatch performed water management using IoT technology, which was the purpose of this study. NTT DoCoMo's network and radio waves were relatively stable even in mountainous areas. Therefore, stable operation was expected in the region as well. In addition, paditch gate 02+ could remotely control and automate the necessary water management after water level measurement and provided a service that enabled water management from a remote location. These products could solve the problems that farmers in terraced rice fields had, which will be described later. The novelty of this study was regarding its focus on the attributes of the subjects.

The agricultural population in rice cultivation was reducing, and the population was aging [8]. As mentioned above, there were many terraced rice fields in the mountainous areas, and the area of one paddy field was not as large as agricultural land. Thus, a large-scale yield could not have been expected. In addition, as the location may not have faced the maintained roadway, there were disadvantages in terms of location, such as the difficulty with inserting agricultural machinery [5]. However, terraced rice fields had various functions, and considering the sustainability from the viewpoint of land use in mountainous areas, it was important to incorporate labor-saving and automation technology to protect the terraced rice fields.

To keep the rice terraces as cultivated land, we thought that it was necessary to pay attention to the bearers and to have a system that matched the attributes of the agricultural population. In most agricultural IoT systems, the information provided was from a web application. However, for elderly people, web applications were often not tools that they used on a daily basis. The proposed system will be described below.

3 PROPOSED SYSTEM

The proposed system considered the network environments of the Otari Village, the Kita-azumi District, and the Nagano Prefecture, which cooperated with the proof-of-concept for this study, as well as the characteristics of farmers in rice terraces. The outline of the system is shown below, and then the details are described for each network, hardware, and software.

3.1 System Overview

Figure 1 illustrates the overview of this study. In the following, the technologies for configuring the system are shown separately for networks, hardware, and software. The paddy field water level monitoring system can be seen in a schematic diagram of this system in Fig. 1 for the terraced rice fields in mountainous areas.

The flow from data measurement to information provision shown in the figure is explained. First, the device that measured the water level and the other data in paddy fields had a built-in communication module with Sigfox and sent data at specified time intervals. Then, the data was sent to the Sigfox backend server, which sent it to the data server that we developed in MongoDB. This data server communicated with the web application server prepared for the web application for users and offered a web page that provided data visualization to each user. Hence, the measurement data, including the summarized information, was sent to the specified e-mail address.

The details of the network, hardware, and software, which are the technologies for configuring this system, are described below.

3.2 Network

For the network, we adopted Sigfox, which had been prepared by the local governments of the Otari Village. Sigfox was one of the LPWA (low power wide area) standards and was a global IoT network featuring low cost, low power consumption, and long-distance transmission [9, 10]. Using the frequency band at approximately 920 MHz of this network, the speed of uplink communication from the terminal to the base station was approximately 100 bps, and that of downlink communication was approximately 600 bps. In addition, the maximum data capacity that could be transmitted in one communication attempt was 12 bytes, the

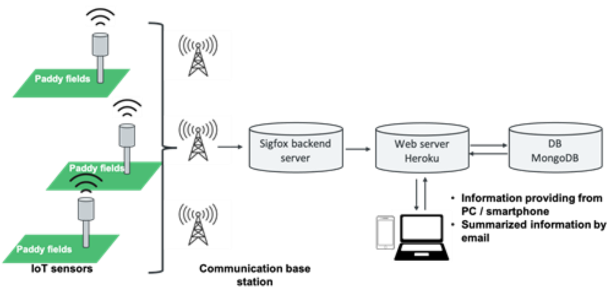

Figure 1 Overview.

Table 1 A list of collected data.

Data	Contents
Water level 1	5 levels (minimum value 3 cm to maximum value 5 cm)
Water level 2	0.5 cm (maximum 12 cm)
water temperature	Paddy water temperature (℃)
temperature	Temperature (℃) approximately 1.2 m from the ground
Humidity	Humidity on the board (%)
Atmospheric pressure	(hPa)
Substrate temperature	Substrate temperature （℃）
Illuminance	0-255 step illuminance
Internal operating voltage	(V)

Table 2 Detailed information of the payload design.

Byte index	Contents
0	Outdoor temperature
1	
2	Water temperature
3	Board temperature
4	Luminance
5	Voltage
6	Air pressure
7	
8	Humidity
9	Water level
10	Empty

upper limit of the number of communication attempts per day was set, and there was a limit of 140 times for uplink and 4 times for downlink.

The details of data selection will be described in the measurement section. This time, the data in Table 1 were acquired, and the payload of the data sent from the hardware to the Sigfox Backend Server was in the format shown in Table 2.

3.3 Hardware

This section describes the network-compatible water level measurement device installed in paddy fields, including the unit of measurement, transmission, and power supply. Figure

Measurement unit

In this system, the water level and water temperature required for water management in paddy fields were collected as important measurement data. We used two devices with different measurement methods. One was a float switch type water level measurement sensor (hereinafter referred to as a float sensor) that determined the water level position by reacting to the reed switch by raising and lowering the float. The other was a float-less switch type water level measurement sensor that measured the resistance value (voltage) between two poles and determined the presence or absence of water [11].

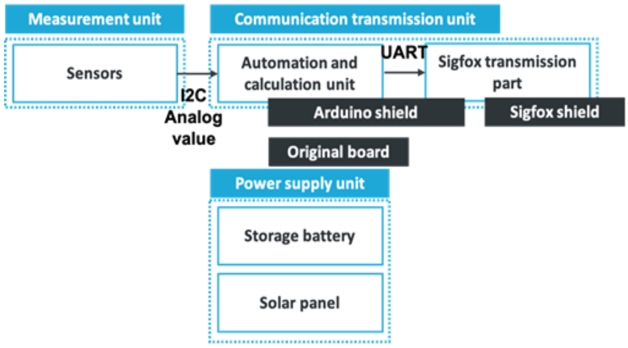

Figure 2 Block diagram.

2 shows a block diagram with the connections between each part and the board.

The hardware was divided into a data communication unit, a measurement unit, and a power unit. The measurement unit mainly measured water level data and environmental data, such as temperature and humidity.

Communication unit

The details of the communication unit are described. The communication unit consisted of an Arduino that performed control and calculation as the main board, a Sigfox shield that performed transmission, and an original board that controlled the power supply unit. The role of the communication unit was from the measurement unit to analog values, and the purpose was to send 9 types of data (Table 1) collected by I2C communication to the Sigfox Backend Server. A Sigfox module that could be connected to the Sigfox network was connected to the transmission unit, and data was transmitted to the data Sigfox Backend Server at the transmission timing and transmission interval specified by the control unit. Table 3 shows the details of the measurement items and the details of each measurement item of the Sigfox payload.

The data transmission timing is summarized below.

- When the water level changed, it was measured every 10 minutes, and data was transmitted when the amount of water level change from the previous transmission value changed by 1 cm or more for the water level sensor and 1 step or more for the float switch.
- Regular transmission: Every 30 minutes

The former was intended to be adopted in this system because it could be produced with a relatively inexpensive configuration, but the measurement interval depended on the size of the module. Therefore, when designing an existing module, the minimum measurement interval was 3 cm. In general, in the individual farmers' paddy field management, we expected that the resolution would be sufficient and proceeded with production. For the latter, the resolution was sufficient for water level measurement with a float sensor, a water level sensor (ASZ-M0917 [12] made by Aszac Co., Ltd.) that realized a measurement interval of 0.5 cm. Two

Table 3 Detailed information of collected data.

Byte Index	Type	Data	Details	Error	Value
0	Int16	temperature	The temperature of the sensor installed at a position approximately 1.2 m above the paddy field	-1270	275 / 27.5 ℃
1	Int8	water temperature	Paddy water temperature Decimal point truncation	-127	27 / 27 ℃
2	Int8	Substrate temperature	Substrate temperature Decimal point truncation	127	27 / 27 ℃
3	Int8	Luminance	0 - 255	-	240 / 240
4	Uint8	Internal operating voltage	Operating voltage of the main IC inside the board, rounded down to the first decimal place	-	50 / 5.0 V
5	Uint8	Barometric pressure	Atmospheric pressure on the board, Rounded down to the first decimal place	65535	10132 / 1013.2 hPa
6※7	Uint16	Humidity	Humidity on the board, Decimal point truncation	255	42 / 42 %
8	Uint8	Water level	6 levels of water level measured with a float switch	255	1 / 1
9	Uint8	Water level	25 levels of water volume measured by water sensor every 5 mm	255	3 / 1.5 cm
10	Uint8	Substrate temperature	The temperature of the sensor installed at a position about 1.2 m above the paddy field	-	-
11	empty	unused	-	-	-

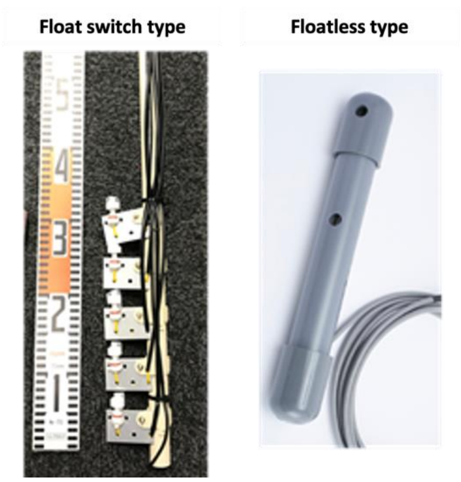

Figure 3 Appearance of two types of water level sensors.

types of sensors were used together. Figure 3 shows the appearance of the two sensors.

In this study, we designed a float sensor-type water level measurement sensor. Float sensors were installed at intervals of approximately 3 cm, and fine adjustments were made at the time of installation where the threshold value was requested. As mentioned above, the minimum value could have been adjusted to approximately 3 cm, but it was possible to register the desired interval of the user in the system. If the interval was 5 cm, the measured quantity was 0 to 20 cm. Next, Figure 4 shows the circuit diagram of the float sensor. The float sensor of S1 in the figure shows the ground side. The resistance value (SUM R1 to R5) changed by grounding in order from S1, and the design enabled identification by the input voltage.

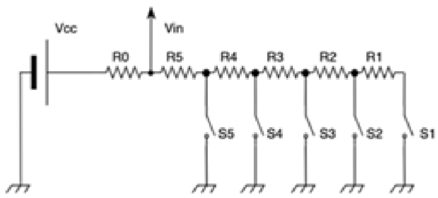

Figure 4 Float sensor input circuit diagram.

Table 4 A table of Analog voltage threshold.

	Measured value(mV)	Theoretical value(mV)	THRSD+	THRSD-
FREE	5000	5000	0	418
S1	4169	4165	418	83
S2	3998	4000	83	125
S3	3758	3750	125	208
S4	3450	3335	208	418
S5	2917	2500	418	2500
FREE	5000	5000	0	418

We collected not only the water level, but also the environmental data, such as water temperature, outside air temperature, humidity, and atmospheric pressure, as well as the state data inside the device (Table 1). The data was necessary for rice cultivation and for utilizing the internal state data of the device. A sensor (DS18B20) was used for water temperature and air temperature, and a sensor mounted on Sigfox's transmission module Una Shield (V2S2) was used for collecting humidity, atmospheric pressure, and substrate temperature data. The illuminance was converted from the input terminal of Arduino, which was capable of an analog input of 0 to 5 V, into 256 steps of 0 to 255 using a diode.

The conversion was an Arduino specification, and the resolution was 19.5 mV. Regarding the illuminance, it was assumed that the timing of sunrise and sunset and the relative shadow when compared with other days would have been used as a reference. Hence, it was not assumed that it would have been converted into a physical quantity that indicated the actual brightness of light. The internal operating voltage was the voltage that operated on the main IC in the Arduino. A voltage of 9 to 24 V was input from the battery to the Arduino, and the voltage was internally stepped down to 5 V. Since the value was the voltage collected in the main IC, 5 V was measured in principle.

Power supply part

The power supply unit used solar panels to generate electricity and a storage battery installed inside the device. It rained for 2 to 3 days after being fully charged. In addition, the solar panel should be installed at a position different from the sensor device. Table 5 showed the electrical characteristics of the solar panel used this time. Table 6 showed the electrical characteristics of the device. Figure 5 showed the appearance of the hardware.

3.4 Software

The abovementioned hardware in a paddy field collected data for paddy field monitoring, such as the water level, and visualized it with a device. The software had three functions as a web application. For example, a smartphone or PC provided an environment where the status of the paddy field could be confirmed, even from a remote location. The following points were developed for the functions of the web application.

1. Periodically collected measurement data from the Sigfox backend server
2. Displayed the measurement data on the web page on user screens
3. Sent the latest measurement data to the specified email address at the specified transmission interval

The function of item (1) was to store data from the Sigfox backend server in a data server prepared in advance. For that, we developed a webhook on the Sigfox backend server side and stored it in the prepared database. A "Webhook" was a mechanism to notify an external service by HTTP when an event was executed in a web application. When new data was stored in the Sigfox backend server, the data was sent to the database at the same time. As item (2) under this function, the DB acquired the latest data and reflected the latest data on the web page from the linked web application server. In addition, as item (3), regularly sending to e-mail would be carried out.

We built the web application server in Heroku, which is a cloud application platform, using Node.js, which is a JavaScript language. In addition, MongoDB, a document-oriented database, was used as a DB for storing measurement data, and data was linked between Heroku and this database using socket communication. In Heroku, we built a front side that presented web pages built using the JavaScript framework, Vue.js, and the CSS framework, Bootstrap. Figure 6 is implemented for the above functions. Table 3 shows the development environment.

Table 5 Characteristics of solar panel

Item	Detailed information
Normal state	12 W
Maximum output power	21.8 V
Open circuit voltage	0.73A
Short-circuit current	17.4 V
Maximum output power voltage	0.69A
Maximum load current	-

Table 6 Characteristics of electrical device.

Item	Use
Storage battery capacity	14000 (mAh)
Input voltage	9～24 (V)
Operating voltage	9 (V)
power consumption	Standby: Approximately 0.36 (W) When sending: Approximately 0.9 (W)
Operating temperature	0-40 (℃)
Storage temperature	-40-85 (℃)

Figure 5 Appearance of designed hardware and setting.

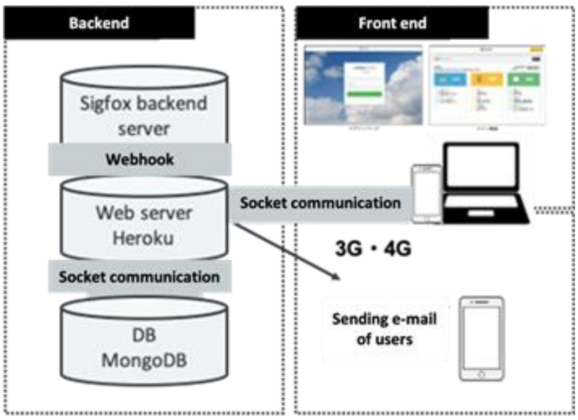

Figure 6 The overview of proposed system.

Table 7 The development environment of the software.

Object	Purpose
Development PC	Macbook
Web application server	Heroku
Data server	MongoDB
Backend and frontend development languages	Node.js
Front-end development language	Vue.js
Bootstrap	CSS framework for front-end development

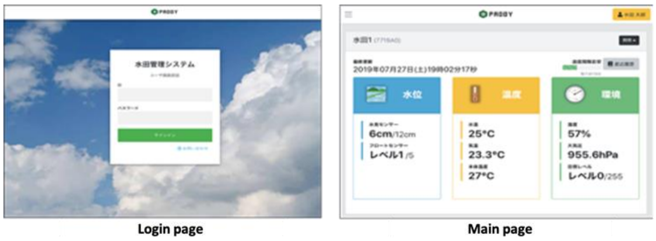

Figure 7 Screen shots of the login and main web pages.

.

Figure 7 shows a screenshot of the actual web page. On the main screen, users could browse data by water level, temperature, environment and category, and the gauge on the right showed the time until new data was sent to the Sigfox backend server. The latest data was reflected on this page.

In addition, this web page design was created from interviews conducted in advance with the experiment participants who were paddy field owners. The participants had an internet environment, had no resistance to digital devices, such as personal computers, smartphones, and tablets, and were willing to use web applications, but selected the types of data to be provided (mainly water level). The water temperature was easily noticeable, and they requested push-type data provision by e-mail notification. Therefore, we implemented a simple design, as shown in Fig. 8, and an email notification function.

E-mail notification

This function inserted the latest data in the database into a premade fixed phrase at the time specified by the user and sent it to the specified e-mail address. This function was executed in Heroku and received by the user through a wide area network, such as 3G/4G.

4 EXPERIMENT

This section describes an experiment for the proposed system. The experiment was conducted in the Otari Village, the Kita-azumi District, and the Nagano Prefecture, for approximately two months from July 12 to September 20, 2019.

The experiment participants were three paddy field owners, devices were installed in each of the three paddy fields, and a total of nine devices were operated. Before and after that, we collected hearings to obtain information related to this system. The information on collaborators, including geographical information, is described Table 8.

In addition, Fig. 7 illustrates the overall positional relationship by plotted in Google Map [13]. From the north, there were the Fukahara, Mushio, and Kurokawa districts. Figure 8 shows the rice terraces in the Otari Village.

Table 8 Information of experiment participants

Number	District	Age	Experiment target paddy field
N	Fukawara	70s	Three
C	Kurokawa	40s	Three
S	Mushio	60s	Three

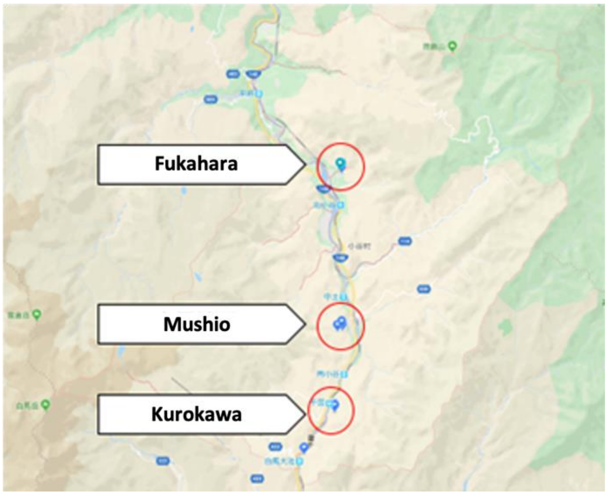

Figure 7 Places of the experiment.

Figure 8 Rice terraces in the Otari village.

5 EVALUATION

This section describes the evaluations collected from the experiments in networks, hardware, and software.

5.1 Network

This section summarizes the radio wave conditions in each area created based on the RSSI values stored in the Sigfox backend server. Figure 9 illustrates the location of the Sigfox base station and each district. Three Sigfox base stations were installed in the Otani Village, and the identification IDs of the base stations were 65B2, 65A3, and 6595. Each base station was installed near the center of the identification ID circle shown in Fig. 9 plotted by Google Map [13].

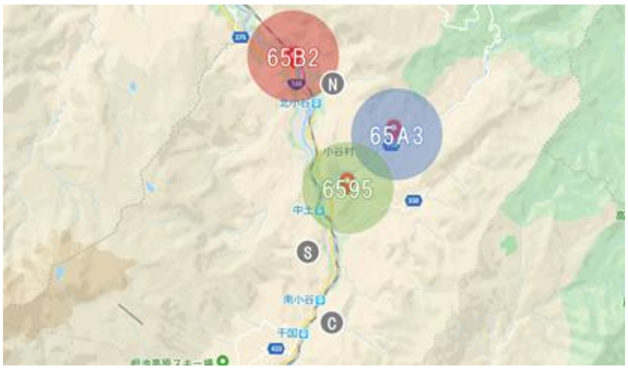

Figure 9 Location of the base stations and the experimental districts.

Although Sigfox had a domestic population coverage rate of 95% in Japan [1], a base station was set up because there were areas where radio waves did not reach the Otari village, which was a mountainous area. Since this system was the first outdoor IoT system installed in the village, this analysis was conducted with the aim of confirming whether the network was working properly. Figure 10 shows the radio field intensity data in the Fukahara area. The frequency of transmission to the base station of 65B2 was shown in the figure. The same analysis was performed in the other two districts, and we found that the frequency of transmission to neighboring base stations was high.

From this result, it was concluded that the network was stable and did not lead to system operation problems, such as data loss.

5.2 Hardware

This section mainly describes the measurement results of the water level sensor data. Figure 11 illustrates all the data measured from the float switch and the water sensor from July 11, 2019, to September 19, 2019 (70 days) in the Kurokawa district C-1. The horizontal axis represented the date, and the vertical axis represented the water level (0 to 15 cm). The amount of water in C-1 was relatively small, and the average value was close to 0. Comparing the value of the float sensor with the value of the water sensor as a reference, it could be seen that the value fluctuated according to the value of the water sensor. However, from 8/5 to 8/7, 8/11, and 8/13, there were some places where the float sensor did not move.

Figure 11 shows that two types of water level sensor's result of sensing data.

5.3 Software

Since the stable system operation was observed in the software, the results were described in the interview based on the questionnaire conducted face-to-face in this evaluation. The data obtained from this system and the usability of the web application are described below.

Data

The three collaborators browsed the web application more than three times per day and were highly interested in the measurement data. The most interesting data were the water level, followed by the air temperature and the water temperature. Since the data on the air temperature and the water temperature could not be confirmed thus far, the collaborators wondered how the data related to the growth of rice. In addition, the atmospheric pressure and the illuminance were not very helpful for cultivation.

Web application usability

The convenience of the web application was highly evaluated from the experiment participants, and the usability was also highly evaluated. However, there was a good point made that the necessary data, such as the display of the maximum and minimum temperatures of the day could be displayed, and that the flexibility of the data display function could be a future issue. In addition, the method of browsing web applications differed depending on the personal computers, tablets, and smartphones. Therefore, a

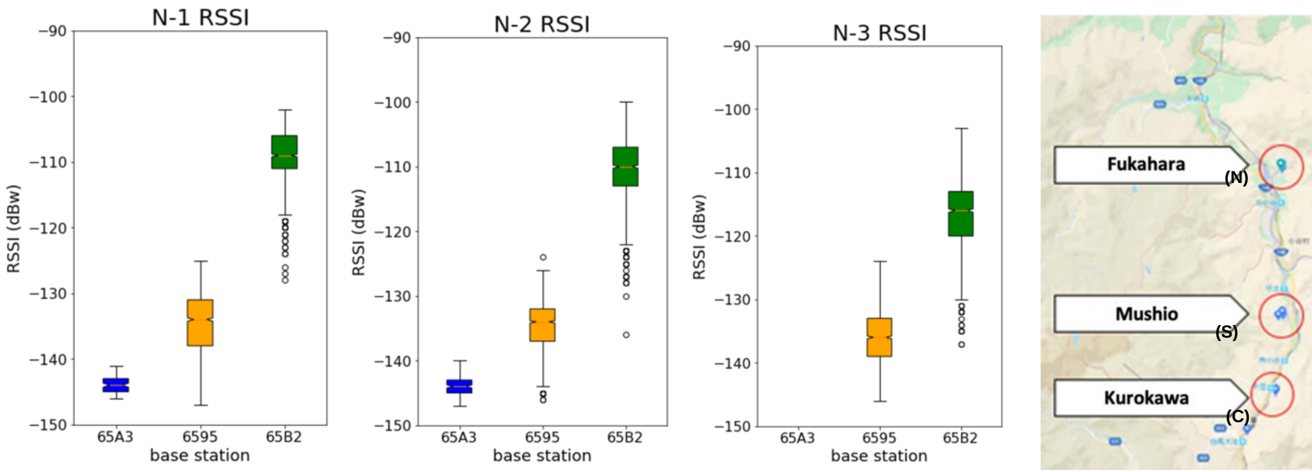

Figure 10 Graphs of RSS values.

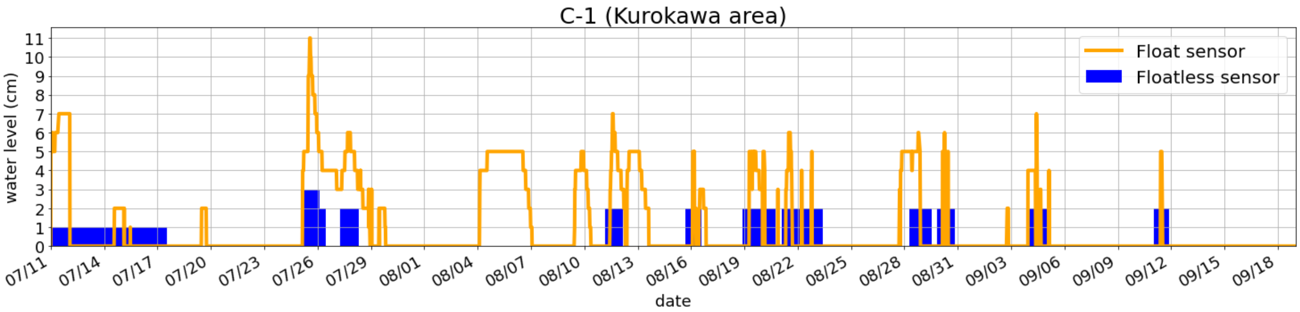

Float sensor

Average	0.2 cm
Maximum	3.0 cm
Minimum	0.0 cm

Floatless sensor

Average	0.2 cm
Maximum	11.0 cm
Minimum	0.0 cm

Figure 11 Collected data from two types of water level sensors.

collaborator expressed that the display was small, and it was considered necessary to make the font size customizable.

Email notification function

For the e-mail notification function, we customized the paddy field managers to provide the most suitable information for each individual. It was the latest information on the three items of water level, water temperature, and temperature, but there was a collaborator who mentioned that the water level was only enough for one of the participants, and the user needed customizable management functions.

5.4 Overall

The purpose of this system was to save labor. The system can support paddy field labors in the point that it provides useful information for confirming the decisions concluded from patrols. Many collaborators expressed that they wanted to grasp the rice growing situation by looking at the state of the paddy field, and it was difficult to provide an effect that exceeded the visual inspection of the rice growing situation from the provision of information. Therefore, remotely providing paddy field information would be useful for them, and if an automatic water level management system could have been connected to our system, the number of patrols by users would have been reduced dramatically.

6 CONSIDERATION

Based on the results of the previous section, this section describes considerations in networks, hardware, and software. In addition, we considered whether the system was designed to be used by the elderly, who were the bearers of rice cultivation in the rice terraces in this study.

First, regarding the network, problems could not be found. Next, regarding hardware, we considered the water level to be the most important part of the data and focused on water level data analysis. As a result, problems were found with each of the float sensors and the water viewing sensor. If this data was unreliable, the value of the entire system would have been lost. Thus, we decided that a review was necessary. However, in this respect, the characteristics of paddy fields varied widely, making it difficult to design hardware that could handle all paddy fields. It would have been necessary to consider how to make it versatile.

In addition, two of the three participants in the experiment were elderly people, and the fact that both understood how to use this system and connected it to the paddy field patrol was useful for the purpose of this system. The evaluation was obtained. In addition, some participants were considering the use of the collected data, though we found that the collected data was expected to be used not only for patrols of paddy fields, but also for the prediction of harvest time and quality control. Therefore, it will be necessary in the future to improve the reliability of the data and organize the functions for providing simple data to farmers.

7 CONCLUSION

In this study, a demonstration experiment using a paddy field water level monitoring system was conducted in the Otari Village, the Kita-azumi District, and the Nagano Prefecture, where Sigfox, which was one of the area networks, could have been used, with the aim of saving labor in paddy field patrols by providing information. The availability of this system was confirmed from the results of the quantitative and qualitative evaluations obtained from the abovementioned demonstrated experiments and hearings.

ACKNOWLEDGMENTS

We would like to express our deep gratitude to everyone at the Otari Village Hall in the Kita-azumi District, Nagano Prefecture, and KCCS Mobile Engineering Co., Ltd. for their great cooperation in this study.

REFERENCES

[1] A.Ushijima, M.Nakazono, “Changes in farming environment and rice terrace conservation in small-scale villages in mountainous areas, ” Architectural Institute of Japan Technical Report Collection.Vol. 23, No.55, pp. 979-984 (2017).

[2] Y.Kawahara, H.LEE, M.M.Tentzeris, “Sensprout: Inkjet-printed soil moisture and leaf wetness sensor,” In: Proceedings of the 2012 ACM Conference on Ubiquitous Computing. 2012. p. 545-545 (2012).

[3] N.Ikeda and et al, “Ground temperature difference driven sensor for environmental monitoring.,” In: Proceedings of the 2018 ACM International Joint Conference and 2018 International Symposium on Pervasive and Ubiquitous Computing and Wearable Computers. 2018. p. 353-356 (2018).

[4] S.P.Kumar, et al. “Smart paddy field monitoring system using deep learning and IoT.” Concurrent Engineering, vol. 29, pp. 16-24 (2021).

[5] A.Muhammad, et al. “Internet-of-Things (IoT)-based smart agriculture: Toward making the fields talk.” IEEE access, vol.7, pp. 129551-129583 (2019).

[6] Japan Cabinet Office, “Office products”. URL: https://office.microsoft.com/en-us/products, Japanese only (2021-06-12).

[7] “paddich”. URL: https://paditch.com/, (2021-06-12).

[8] “Basic policy on promotion of terraced rice fields”. URL: https://www.kantei.go.jp/jp/singi/tiiki/tanada/pdf/tanada_kihon_housin.pdf, Japanese only (2021-06-12).

[9] “Promotion of the terraced rice fields”. URL: https://www.maff.go.jp/j/nousin/tanada/tanada.html, Japanese only (2021-06-12).

[10]Z.C.Juan. et al. “Sigfox system description,” LPWAN @ IETF97, Nov. 14th (2016).

[11]T.T.Duc, M.Mizoguchi, Y.Kawahara, T.Asami, “Error Reduction in Capacitive Based Water Level Sensor for Paddy Field,” Shingaku Sodai 2016, B-18-16, March (2016).

[12] “Water level sensor (water level detection / detection / measurement)”.URL:http://www.asuzac-pd.jp/seihin/mizumisensa.htm, Japanese only (2021-06-12).

[13]Google Map, https://www.google.co.jp/maps/ (2022-11-30).

(Received: November 16, 2021)
(Accepted: December 23, 2022)

Kazuma Nishigaki

He was graduated from school of information environment, Tokyo Denki University as a bachelor. Also, he is a master student at Graduate School of Informatics, Tokyo Denki University, Japan. His expertise is development of IoT applications.

Naohiro Kamatani

He was graduated from school of information system engineering, Tokyo Denki University as a bachelor. Also, he is a master student at Graduate School of Informatics, Tokyo Denki University, Japan. His expertise is development of STEAM Education Contents.

Kanae Matsui

She is an associate professor in School of System Design and Technology, Tokyo Denki University. She has Ph.D. degree from Graduate School of Media Design, Keio University. Her expertise is to study smart city platform and IoT application.

Industry Paper

Proposed Small Observation Rover with Six In-wheel Motors for Precision Agriculture

Kenji Terada*
Masaki Endo*, Takuo Kikuchi*, Shigeyoshi Ohno*
* Division of Core, Polytechnic University, Japan
{k-terada, endou, kikuchi, ohno}@uitec.ac.jp

Abstract - Japanese agriculture is confronting the simultaneous difficulties of an aging population, diminishing numbers of workers, and increased area of arable land. Therefore, smart agriculture using IoT and robots is attracting attention. As a crop condition observation technology, UAVs have been attracting attention. Nevertheless, observing pests and diseases under leaves is impossible, although that is the main avenue of crop damage. Therefore, we propose a small agricultural rover that can provide above-ground images of leaf undersides and environmental information that can support important decision-making for precision agriculture. This paper describes the structure of a small agricultural rover that can provide stable observations for sustainable crop production in an orchard.

Keywords: agriculture, IoT, robot, sensing

1 INTRODUCTION

Undoubtedly, agriculture is an important economic sector worldwide. However, the Japanese agricultural sector particularly is confronting the difficulties of an aging population and a severe labor shortage. As numbers of agricultural enterprises continue to shrink in Japan, the average amount of arable land per farmer is expected to expand [1]. Therefore, great interest has arisen in smart agriculture systems. Farmers must increasingly use the internet of things (IoT) and robot technology to acquire and analyze highly accurate data related to diverse crop production factors to realize precision agriculture [2]. These demands have hastened the development of useful farm machinery [3 - 4].

Particularly, AI-based systems are finding new value in agricultural management. Currently, a cloud service that uses sensors to measure environmental conditions to predict harvest and disease outbreaks is in practical use [5]. For example, services worldwide assess disease damage from images of plants taken by farmers with smartphones and other devices [6 - 9]. An inexpensive system that uses crop images to monitor crop growth is expected to increase agricultural efficiency. It is also expected to reduce the risk of crop failure in areas where there are few skilled farmers. In another study, remote sensing technology using an unmanned aerial vehicle (UAV) is used to monitor growing conditions through images. With the advent of UAVs, it has become easier to collect data to support farm growth management [10]. However, estimating growing conditions from aerial images taken by UAVs requires ground-truth: actual measurements. Moreover, aerial photography by UAVs is not a panacea. Ground observations are necessary (Fig. 1).

Figure 1: Diseases and pests on the leaf underside.

Figure 2: Virus carrier on the leaf underside on farms owned by co-developers.

For example, disease detection from imaging requires visual evaluation such as observation of a single leaf on the ground for early detection of diseases such as powdery mildew on the underside of leaves [11]. These observations are limited to those made from the air. Various crop-damaging pests are parasites that feed on the underside of leaves: lepidopteran pests, coleopterans, spider mites, and snails [12]. If even one virus-diseased plant is missed, an infection might spread to other crops on the same farm, leading to secondary damage. Virus carriers are insects, mollusks, or fungi that parasitize leaf underside (Fig. 2).

The Ministry of Agriculture, Forestry, and Fisheries of Japan report that efforts to prevent the spread of plant diseases and pests can contribute to SDGs 1, 2, 8, 12, 13, 15, and 17 [13]. The amount of damage caused by such diseases is said to exceed 100 billion yen per year [14].

Herein, we propose a small agricultural rover able to observe environmental data and the undersides of crop leaves from the ground to observe crops and manage field variation, which is important for precision agriculture.

The capabilities necessary to make observations using a small rover are the following.

- Driving on uneven terrain with branches and irregular soil composition, topology, and texture
- Collection of environmental parameters such as leaf underside images, temperature, and humidity. while driving between rows of crops
- Use of field maps using data from observations

Observation by a mobile rover is an effective means to achieve low-cost ground observation of the leaf underside for each crop. Observing leaf undersides requires a rover that can suppress rover swaying caused by various small bumps inherent to farms, such as branches and tread marks. Therefore, the small agricultural rover developed for this study of an orchard has a mechanism with a damper function in the frame body to which the wheels are attached.

For the reasons described above, this study proposes a small agricultural robot that observes the soil and which also takes upward-looking images of crops on a farm to complement agricultural management data obtained from drones and farmers. Section 2 presents explanations of related studies and the position of this study among the relevant literature. Section 3 presents a description of a prototype developed for this research. Section 4 gives the results of prototype driving tests. Section 5 presents the conclusion.

2 RELATED WORK

For this study, the name of the small robot to be developed is the Field Scouting Rover (FSR). Robots of many types patrol farms [15 - 18]. Actually, FSR aims at achieving stable autonomous running on uneven terrain, despite its small size, for close observation of many crops.

As ideas we propose, we consider that an important issue for agricultural robots is the decline in maintenance performance caused by miniaturization. Especially, the aging of the workforce requires not only the easy operation of robots but also easy maintenance of machines. Also, uneven terrain is a necessary part of farm driving. Replacing dampers and other parts used in many agricultural rovers to cope with uneven terrain is a highly specialized task. Therefore, we specifically evaluated a mechanism with a damper function in the frame itself, where the wheels are mounted, to improve ground contact on mildly uneven terrain without increasing the number of parts. This mechanism mitigates the vehicle body's vertical movement and angle changes by connecting all wheels with links (Fig. 3).

Furthermore, to distribute the load, the number of wheels was increased from four to six, which is the number of wheels used in many agricultural robots. Thereby the running performance was improved and tire marks on the farm were reduced. Moreover, the number of parts was reduced by omitting the steering mechanism. This feature particularly addresses a farm's need to travel in straight lines rather than making sharp turns.

The rocker-bogie mechanism used in the Mars explorer is famous as a similar idea. The rocker-bogie mechanism structure can apply an equal load to each wheel, which enables stable operation, even on uneven terrain. However, because of that rocker bogie mechanism structure, a vast difference exists in running performance between the front and rear. Additionally, it has been pointed out that the number of parts increases along with the need for lower height: it is not a simple mechanism [19]. Therefore, the FSR frame has a six-wheeled vehicle mechanism that differs from the rocker bogie mechanism. The rolling mechanism allows the FSR to maintain contact between the ground and the six wheels even when the ground is uneven on both sides. The other mechanism used for reference uses in-wheel motors that are driven separately. Steering is done by differential movement of the left and right wheels [20]. The FSR uses no damper or other complicated parts for the linkage mechanism.

Figure 4 presents the FSR position in farm observations. Observations made by small robots will enable farmers to make better-informed farm management decisions using precision information that is obtainable remotely. If a good farmer observes disease or insect damage in one place, then the farmer will then inspect several places and make a comprehensive judgment.

The FSR is aimed at complementing data obtained by UAVs that make observations from the sky. Thereby, the FSR can observe areas that are difficult for farmers to see, but which farmers must observe, such as crop bases and leaf undersides. FSR is also expected to be used to observe crops near the farm using thermometers, hygrometers, and barometers. Therefore, the FSR will be equipped with a camera for real-time crop observation. The situation can be checked with a smartphone or other device by streaming and storing crop images. The sky will occupy most of the background when the rover looks up at the crop leaves. The amount of background information unrelated to the plant can be reduced. The problem with plant disease diagnosis is that operational performance cannot be ensured for images taken in a different environment because of overtraining that includes background information, which occupies a larger area than that of the plant [21]. By reducing the number of useless background images, the analysis time can be reduced.

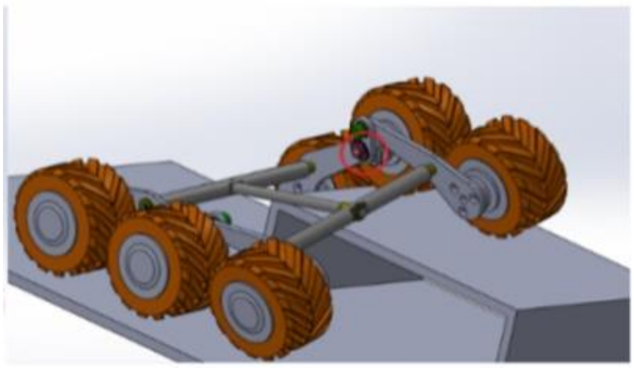

Figure 3: Frame design.

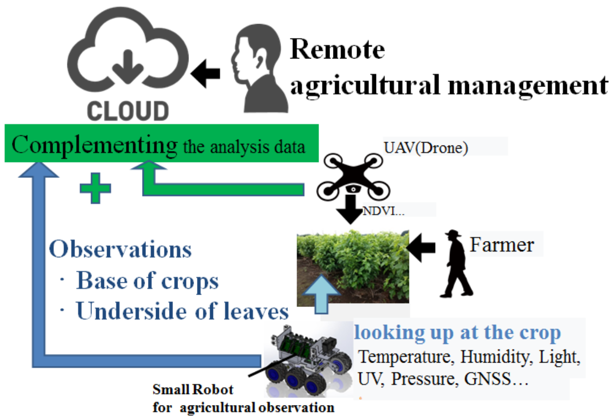

Figure 4: Positioning of FSR for agricultural observations.

3 ROVER DEVELOPMENT

3.1 Specifications of FSR

Table 1 present the FSR specifications. Fruit trees, especially those that use leaves such as mulberry and tea, are harvested once a year. These crops must be observed daily to maintain quality. Spacing between fruit trees in a small orchard is 1,000 mm [22]. From the top, the FSR is the size of an A4 size paper with six wheels. The FSR size is intended to be sufficiently large to observe these crops. Increasing the road-following ability makes it possible to drive stably without the tires floating. An effective way to increase the road-following ability is to make the wheels heavier. The FSR has an in-wheel motor with a built-in motor mechanism. The motor weight increases the wheel weight. The in-wheel motor used for the FSR was selected from commercially available products that can be procured easily. We selected the in-wheel motor for the FSR from commercially available products that were procured easily. The two main points were that the motor should support only one side of the wheel (cantilever) and that it should have sufficient torque to tow its weight to realize the mechanism used in the FSR. We selected parts from a battery-powered E-Skateboard. The frame size was designed based on the selected in-wheel motor diameter. It was sufficiently large to observe an orchard farm.

3.2 Frame of the Body

A frame with an in-wheel motor was designed using " SolidWorks Corporation," as depicted in Fig. 5, after the design, the software simulator was used to check the grounding characteristics. Parts of the frame were fabricated using numerical control machining and a laser machine.

3.3 In-wheel Motor Control

Figure 6 shows the in-wheel motor control circuit. The driver circuit that came with the in-wheel motor could not connect to other electronic circuits. Therefore, we built a circuit using a brushless DC motor driver (TB6605FTG). The in-wheel motors on the market varied in terms of weight and the number of coil turns. In addition, individual speed control is necessary to achieve straight line operation [20]. A microcontroller for in-wheel motor control was provided for each in-wheel motor. The FSR's control microprocessor uses a Jetson Nano. The control circuit is connected to a 2D-LiDAR [RPLIDAR A2M8; Shanghai Slamtec Co. Ltd.]. The 2D-LiDAR enables the detection of obstacles among the surroundings of the FSR. The control microcontroller was constructed to send rotation commands to the microcontroller, which controls each in-wheel motor. To enable BLE communication with smartphone applications, as described in Section 3.5, the microcontroller for control is connected to the BLE module [BLE Serial3]. In addition, the control microcontroller is connected to the gyro sensor [CMPS12], which is located at the center of the FSR's chassis for angle control of turning and other operations. For communication between microcontrollers, microcontrollers use I2C communication. One battery was used for each of the two in-wheel motors to enable testing of the individual motor controls and to facilitate testing of flexible layout adjustments in the FSR. In addition, one battery was used for each of the seven microcontrollers. A Li-Fe battery material was selected: it is lighter and safer than Li-Po. Compared to Li-Po batteries, Li-Fe batteries are formed from materials that are extremely resistant to ignition, making them effective for robots with high vibration. The speed of the FSR for observation was set to 3.2 km/h, which is regarded as a slow human gait [23]. Because the selected in-wheel motor was not designed for low speed, the control microcomputer program had to reduce its responsiveness. Therefore, the program to lower the clock of the timer interrupt used for feedback control in the control microcomputer program made it possible to reduce the motor speed.

Table 1: Specifications of FSR

FSR Length [mm]	350.0
FSR Width [mm]	294.0
FSR Height [mm]	310.0
FSR Weight [kg]	7.4
Wheel diameter [mm]	65.0
Wheel weight [g]	760
Maximum power [kW]	0.5[*2] × 6[*1]
Maximum velocity [km/h]	30.3[*2]
Minimum velocity [km/h]	2.4[*2]
Average uptime [min]	63.3[*3]

[* 1] Number of motors
[* 2] motor catalog data (over-engineering)
[* 3] no load

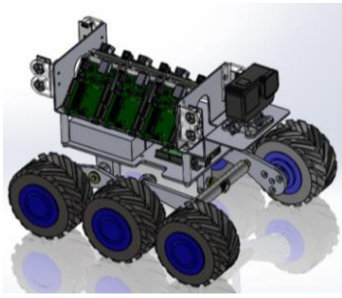

Figure 5: Design and simulation of FSR.

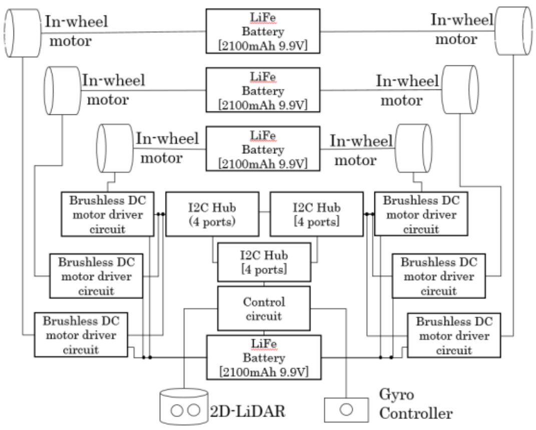

Figure 6: In-wheel motor control system of FSR.

3.4 Log of Environment Sensor Recording Functions

Figure 7 presents a log of FSR environment sensor recording functions used to detect environmental data such as temperature and humidity while taking leaf underside images when driving between rows of crops. Cloud services can collect and store such data. Therefore, sensor connection points must have microcontrollers that can connect to the internet easily. Therefore, the FSR's sensing microprocessor uses a Raspberry pi4 B+. To obtain environmental information on date and time, temperature (°C), humidity (%), light (lx), U-V index, pressure (hPa), and noise (dB), the FSR uses an environmental sensor (2jcie-bl01; Omron Corp.). The sensor can connect the FSR's sensing microprocessor via BLE communication. Thereby, the sensing microprocessor location on FSR can be changed flexibly. To obtain crop images, the sensing processor is connected to a Raspberry Pi HQ Camera. In addition to obtaining the observation location coordinates, the sensing microprocessor is connected to a GPS Module (Ultimate GPS Breakout - 66 channel w/ 10 Hz updates – Version 3; Adafruit Inds.). The program used for observations was produced using Python. The measured environmental information is saved in a CSV file in the sensing microprocessor. Additionally, it uses IoT Core, S3, DynamoDB, OpenSearch Service, etc., which are services of Amazon Web Services, Inc. (AWS), to upload a group of sensor values to a cloud service. The use of cloud services makes remote data observation possible. The sensing microprocessor is installed with a mjpeg-streamer to capture images and distribute images during observation for viewing on a web browser such as a smartphone. Using mjpeg-streamer, one can distribute video and acquire still images using the HTTP protocol. By observing log data gathered by FSR with the program, one can obtain environmental sensor data for crops.

3.5 Smartphone Application to Operate FSR

Figure 8 depicts a screenshot of the smartphone application to operate the FSR. An Android OS smartphone application controls the FSR. The camera image of the sensing microprocessor is projected at the top of the smartphone application screen: a web browser screen. After the user taps the connect button to start communication with the FSR and communication starts, the user can command the FSR to operate by pressing the respective arrow buttons. The FSR stops when the arrow button is released. To experiment with turning the prototype, pressing the automatic button will make the FSR turn when going straight, up to the length (m) entered.

4 EXPERIMENT

It is necessary to verify whether our proposed simple frame with a small number of parts is useful to observe farms.

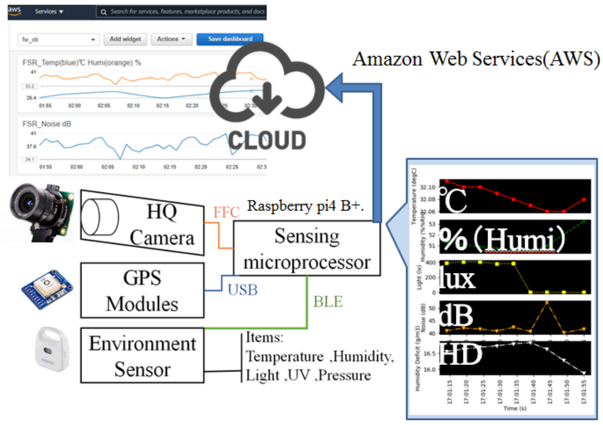

Figure 7: Log of environment sensor recording function of FSR.

Figure 8: Smartphone application to operate FSR.

As described in the *Introduction*, we conducted “Mobility” and “Driving on uneven terrain” experiments to assess driving on uneven terrain with branches and irregular topology. Moreover, a "leaf underside observation" experiment elucidated capabilities for detecting temperature, humidity, and other environmental parameters, along with leaf underside images while driving between rows of crops. Moreover, a field map was produced using observation data.

4.1 Mobility

The FSR is not equipped with a mechanism, such as a constant velocity joint, to change the wheel angle. Figure 9 portrays the FSR movement on a farm. First, to realize stable observation on a farm, FSR needs straight-line control. It also needs control to change the turning radius according to the size of the crop being grown on the farm. Turning is achieved by speed differences between the left and right wheels. Therefore, we analyzed those characteristics during turning by controlling the in-wheel motor speed.

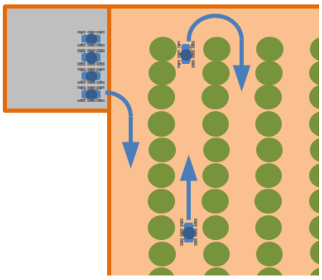

Figure 9: FSR in action on a farm.

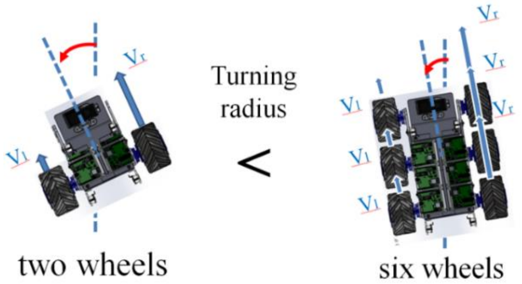

Figure 10: Turning radus of two wheels and six wheels.

Basic characteristics of the turning radius are described in the six-wheeled vehicle model simulator described in one report [24] and the turning method for multi-wheeled vehicles described in another report of the literature [25]. According to those earlier studies [24] and [25], given a greater number of wheels of the driving unit and sufficiently large ground area, then resistance during turning is greater, as is the turning radius (Fig. 10). For two wheels, the turning radius is the distance between the centers of the left and right tire widths when only one wheel is turned. The calculated value is 110 mm if one calculates the turning radius based on the FSR size. In reality, the turning radius will be larger because the ground resistance of FSR with six wheels is greater than that of two wheels.

To measure the turning radius repeatedly for the experiment, we used a board floor, which ensures more level ground than on soil, such as on a farm. We sent a left turn command from our smartphone application and drove until the FSR turned 90 degrees. The speed settings for each wheel were 100 min^{-1}, which is the minimum speed at which the prototype can drive. The speed at which it stops was set to 0 min^{-1}. However, the wheels are not braked. Therefore, the wheels will turn if an external force is applied. Table 2 shows the turning radius resulting from the difference in the way the left and right wheels turn. The measured values in Table 2 are average values of 10 measurements in each case. The case of the spin turn caused by driving with all left wheels backward and all right wheels forward was excluded because it rotates around the chassis.

From the cases shown in Table 2, one can select a useful movement method for turning. The method in case 1 operates only one wheel. The turning radius value of case 1 was 2,134.4 mm. The radius required for turning among fruit trees varies. General fruit tree spacing is 4,000 mm [26].

Table 2: Turning radii of different left and right wheel turn modes (fixed rotation speed of the left wheel)

	Pattern	Average turning radius [mm]
case 1	Right Wheels: forward Left Wheels Front, Middle, Rear: stop	2,134.4
case 2	Right Wheels: forward Left Wheels Front: stop, Middle, Rear: back	2.6 Near spin turn
case 3	Right Wheels: forward Left Wheels Front, Rear: back Middle: stop	3.2 Near spin turn
case 4	Right Wheels: forward Left Wheels Front, Middle: back Rear: stop	2.1 Near spin turn
case 5	Right Wheels: forward Left Wheels Front, Rear: stop Middle: back	145.3
case 6	Right Wheels: forward Left Wheels Front, Middle: stop Rear: back	457.7
case 7	Right Wheels: forward Left Wheels Front: back Middle, Rear: stop	121.0

Case 1 was found to be sufficiently operational as an orchard turning radius. However, spacing between fruit trees in a small orchard is 1,000 mm [22], making it difficult to operate with the turning radius of case 1 operation.

The salient point, as shown for cases 2–7, is that we conceived a method to reduce the turning radius: we drive the left wheels, actually, three wheels, backward when turning left. Cases 2–4 had a turning radius close to that of a super new land turn. The common feature was that two wheels on each side were driven backward. Therefore, after we chose the rotation pattern to be used for turning from cases 5–7, we measured the angle change during rotation in case 5–7 patterns using the gyro-sensor attached to the FSR. Figure 11 portrays a graph of the change in rotation angle for cases 5–7. The horizontal axis is the time spent for a 90-degree turn. The vertical axis is the angle measured by the gyro sensor. In case 6, the return of rotation is large. It can be confirmed that it shakes during rotation. We assume that this large rotation occurs because the battery is located behind the FSR. Therefore, the center of gravity is behind it. We expect the slippage to be large and expect that shaking occurred. If the oscillation is large, then stable observations such as those by image recording by the camera cannot be expected. Therefore, it is necessary to select case 5 and case 7 for observations. For this study, case 7 was used to ascertain whether the turning radius increases because of the speed difference between the left and right wheels. Table 3 presents results obtained from increasing the rotation speed of the right wheel in the rotation pattern of case 7. Increasing the rotation speed of the left wheel caused a larger

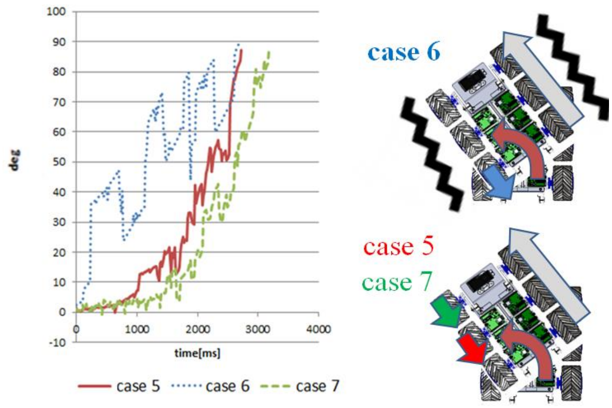

Figure 11: Change in rotation angle during FSR rotation.

Table 3: Turning radius associated with different turning of the left and right wheels (fixed right wheel rotation speed)

	Pattern	Average turning radius [mm]
case 7-1	Right Wheels: forward (100 [min^{-1}]) Left Wheels Front: back (110 [min^{-1}]) Middle, Rear: stop	152.6
case 7-2	Right Wheels: forward (100 [min^{-1}]) Left Wheels Front: back (120 [min^{-1}]) Middle, Rear: stop	176.4

turning radius. Through these experiments, we were able to find a way to change the FSR turning radius. Subsequently, turning was performed on soft soil using case 1 in Table 2. The turning radius was 1,962.9 mm (91.9% of the turning radius of the floor). Wheel slippage was observed. In case 7, slippage was then observed on the left front wheel driving backward. The measured value was 100.2 mm (82% of the turning radius of the floor). To counteract slippage, the ground contact area of the wheels must be reduced, as in ordinary vehicles. For that reason, the wheel tire width must be narrowed.

4.2 Drive on Uneven Terrain

It is necessary to evaluate whether the FSR frame will allow the vehicle to be stable on uneven terrain while driving. Figure 12 shows a test course with a 30 mm step used to verify that the FSR can maintain the same level of wheel contact as in the CAD simulation. The step is set at 30 mm because the FSR is calculable to overcome heights up to half of the tire diameter because of the link structure design. The FSR ran at the same speed as the mobility experiment. On the course, the convex part is blue. The concave part is red. As a result of visual checking of the ground contact, FSR confirmed that the six wheels were installed on bumpy ground (Fig. 13).

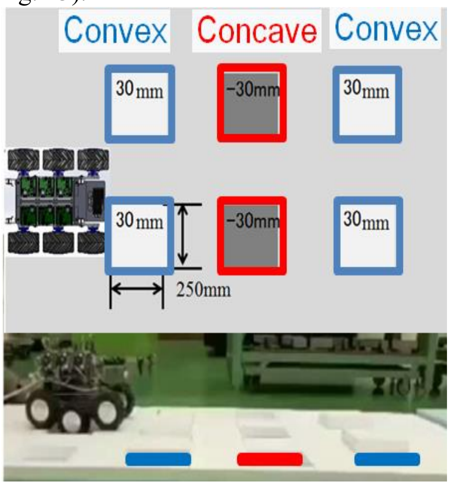

Figure 12: Ground contact performance on a test course with 30 mm bumps.

Figure 13: Driving of FSR with high grounding capacity.

Figure 14: Driving the FSR on the uneven farm.

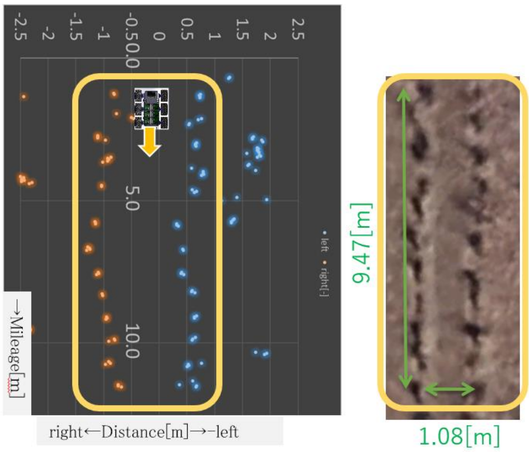

Figure 15: Measurement of tree position (left, measurement result; right, actual orchard).

The FSR was driven in a mulberry field to evaluate driving on uneven terrain (Fig. 14). The FSR used 2D-LiDAR to measure the distance of fruit trees and avoid fruit trees while driving. To detect the fruit tree position, the distance of fruit trees on either side of the FSR was measured. Figure 15 shows the measurement results. The FSR meandered as it took measurements, which distorted the measurement results. Nonetheless, results demonstrated that actual tree positions in the field were identifiable from the tree data.

We confirmed that the FSR obtained good driving performance on a field with numerous small obstacles such as pebbles and branches.

4.3 Observation of Leaf Undersides

Facilitated by the advancement of artificial intelligence (AI, especially machine learning) technology, many research results have been reported [27]. To build a practical system, pre-processing is necessary to judge the recorded crop images properly before analysis by machine learning. Images are taken over a wide area to obtain numerous images from fixed-point observations.

The training data used in the discriminator are diagnostic images from a single leaf, as represented by Plant Village, a well-known dataset on leaf diseases. More is learned from wide area photographs, and lower accuracy of identification is obtained for different farms. Therefore, pre-processing is necessary to extract a single leaf from a wide area photo.

In addition, regularization, such as data augmentation and dropout, is effective as a method to suppress overlearning. Background removal is also effective before regularization.

In FSR observations, one can observe the underside of leaves, whereas the sky occupies most of the background by close observation while moving the crop. By reducing the number of useless background images, the background removal process can be shortened. Furthermore, by correlating the RTK-GNSS coordinates with the acquired images, one can photograph only those areas where disease or insect damage is detected.

In this experiment, the images observed by looking up are sent to an AI-based image discrimination application for discrimination. If one can make no determination, then the background can be deleted to verify whether a correct decision can be made.

Using sensors embedded in the FSR, we experimented to observe whether pests and diseases are visible from the observation results. Table 4 presents observation results obtained for the mulberry farm. For the diagnosis of diseases and insects, we used PlantMD [28], an AI-based smartphone application that estimates diseases and pests from images. Mulberry trees on the farm were photographed from above. Rows of trees without disease were selected. We drove the FSR along the side of the crops and looked up to observe them. After sending the acquired images to PlantMD for diagnosis of pests and diseases, we checked the location at which we obtained powdery mildew detection results. Nevertheless, no powdery mildew symptoms were found (Fig. 16). Powdery mildew causes white spots on the leaf surface. When images were checked, we were able to observe that the leaves had spots through which light shone because of backlighting. We presumed that these points were misdiagnosed as powdery mildew.

Therefore, background removal was achieved using a web service (remove. bg), with foreground extraction using an

Table 4: Observation results for the mulberry farm

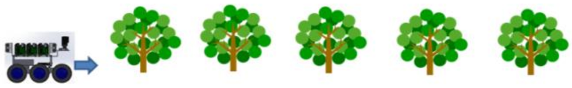

Observed image					
Pests and diseases by the system	powdery mildew	powdery mildew	aphid	aphid	yellow spot virus
Visual confirmation	un-observation	un-observation	observation	observation	observation

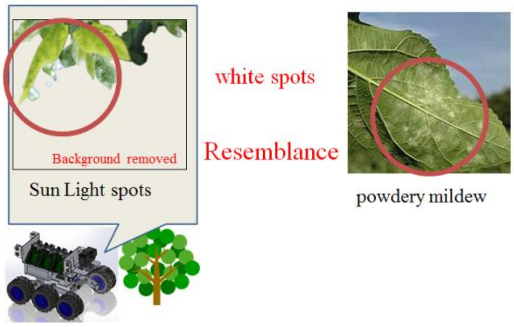

Figure 16: No powdery mildew symptoms.

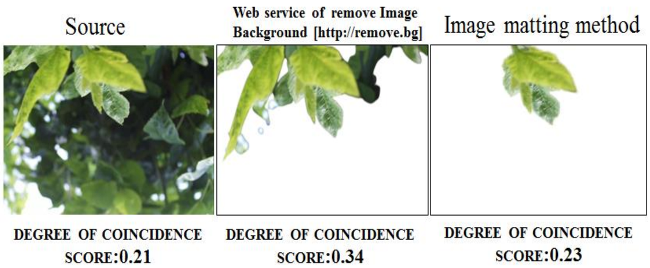

Figure 17: Match score under background removal.

Alpha Matting technique. PlantMD, which can measure disease concordance (Fig. 17), was used to measure the score for powdery mildew. Figure 14 presents the results. All of the diseases were diagnosed as powdery mildew. The effect of the background was determined as minimal. During operation, it is necessary to find a threshold of the detected scores and to consider new powdery mildew detection methods.

We then obtained aphid detection results from two locations. We confirmed the presence of aphids by checking the observed sites directly. Additionally, we observed a yellowing virus disease from one location. Direct confirmation of the area in which the virus was observed revealed a yellow discoloration. However, viral diseases are difficult to assess accurately because they require specialized analysis. Insect damage, however, is easy to detect even by people without specialized knowledge, allowing for rapid eradication of pests.

In addition, the duration of observation within the orchard was measured. Figure 18 shows the mulberry farm size and the number of rows of trees used for observation. FSR drove between the rows of trees from the bottom of the first row to the top of the seventh row in the mulberry field shown in Fig. 18, recording temperature and humidity along with images of leaf undersides. The measurement duration was 2 min and 10 s. The observed data are presented in Figs. 19 and 20. The heat map facilitates easy identification of observation locations.

5 CONCLUSIONS

This study revealed that FSR has the potential to provide crop-specific observation information necessary for decision-making in precision agriculture while driving between crops. The FSR has a simple configuration with a frame that has an in-wheel motor and a linkage mechanism. Nonetheless, the FSR can run on uneven terrain with branches and soil irregularities. We discovered the possibility of detecting environmental values such as leaf underside images, temperature, and humidity while driving between rows of crops by the FSR.

Additional accuracy is necessary for driving and observation locations. The FSR can produce observations of crop variation and can support farmers' decision-making by showing data for locations within their farms.

Future work includes developing a method for pest and disease prediction and detection based on observed images of pests and diseases, time, temperature, humidity, and other observed values obtained using detection technology. Furthermore, to enable autonomous operation, a patrol function based on longitude and latitude information from Camera, LiDAR, and RTK-GNSS is required. It must meet technical standards for automatic operation set by the Ministry of Agriculture, Forestry, and Fisheries [29].

ACKNOWLEDGMENTS

We would like to express appreciation to Professor Kaori Fujinami of the Tokyo University of Agriculture and Technology for expert advice on our research.

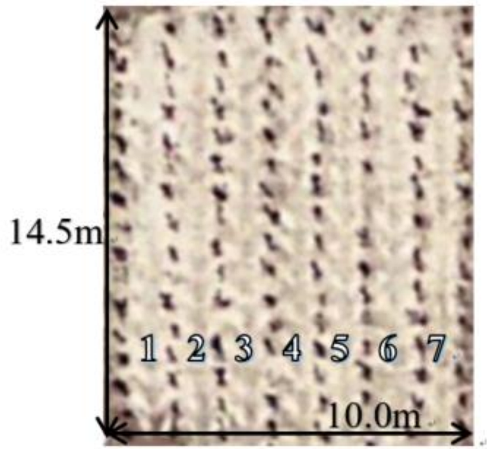

Figure 18: Dimensions and number of trees on the orchard.

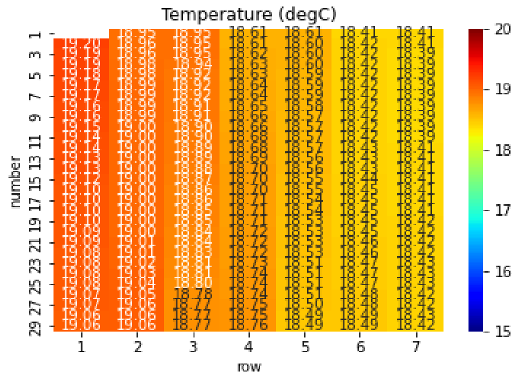

Figure 19: Heat map of orchard temperature.

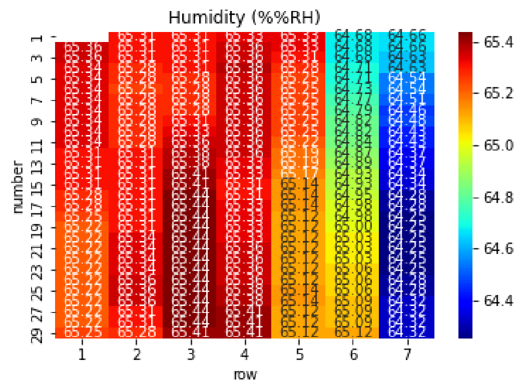

Figure 20: Heat map of orchard humidity.

REFERENCES

[1] Statistics of Agriculture, Forestry and Fisheries, MAFF, pp. 11-7 (2020).

[2] E. Shibusawa, “Precision Agriculture”, Asakura Publishing Co., Ltd.(2006).

[3] J. Champ, A. Mora-Fallas, H. Goëau, E. Mata-Montero, P. Bonnet, “Instance segmentation for the fine detection of crop and weed plants by precision agricultural ro-

bots," Applications in Plant Sciences, Vol. 8, No. 7 (2020).
[4] O. Spykman, A. Gabriel, M. Ptacek, M. Gandorfera, Farmers' perspectives on field crop robots – Evidence from Bavaria, Germany, < https://www.sciencedirect.com/science/article/pii/S0168169921001939 > ,[referred May 2021].
[5] "midori cloud (in Japanese)", < https://info.midori-cloud.net/vision/>,[referred May 2021].
[6]] H. Iyatomi, "Trends and Challenges of Automatic Diagnosis Techniques for Plant Diseases," Japanese Neural Network Society Journal, Vol. 26, No. 4, pp. 123–144 (2019).
[7] D. Mhlanga, Artificial Intelligence (AI) and Poverty Reduction in the Fourth Industrial Revolution (4IR). Preprints 2020, 2020090362 (doi: 10.20 944/ preprints-202009.0362.v1). (2020).
[8] "SCIBAI (in Japanese)", < https://www.mirai-scien.com >, [referred May.2021].
[9], N.S. Naik, V.V. Shete, and S.R. Danve, "Precision agriculture robot for seeding function," 2016 International Conference on Inventive Computation technologies (ICICT). Vol. 2. IEEE(2016).
[10] R. Sugiura, "Remote sensing for large-scale field information using drone imagery," Research Center for Agricultural Information Technology, pp. 184–187 (2020).
[11] S. Yamamoto, "Fundamental Study on the Collection of Big Data for the Agricultural Community Using Machine Vision: Exploring a Potential Technology to Complement Drone Information for Monitoring Plants," Akita Prefectural University Web Journal B, pp. 85–90 (2018).
[12] Ministry of Agriculture, Forestry and Fisheries, pest control,<https://www.maff.go.jp/j/seisan/kankyo/hozen_type/h_sehi_kizyun/attach/pdf/aki3-15.pdf>, [referred Oct .2021].
[13] Changes and Issues Concerning Plant Protection, <https://www.maff.go.jp/j/syouan/syokubo/keneki/attach/pdf/arikata-14.pdf >, [referred Mar.2021].
[14] K. Oshima, "Plant potyvirus evolution the survey of the genetic structure of populations," Virus, Vol. 2, pp. 151–160 (2012).
[15] M. Arun et al., "Smart Agriculture Robot," International Journal of Pure and Applied Mathematics, Vol. 119, No. 15, pp. 1901–1906 (2018).
[16] "avo", <https://www.ecorobotix.com/en/avo-autonomous-robot-weeder/>, [referred Mar.2021].
[17] "Weed Whacker", < https://www.odd.bot/>, [referred Feb.2021].
[18] "DICK", <https://www.smallrobotcompany.com/>, [referred Oct.2021].
[19] A. Schafer et al., "Robot Mobility Concepts for Extraterrestrial Surface Exploration," IEEE, Aerospace Conference, pp. 1–12 (2008).
[20] Y. Hirota, Electric vehicle engineering (in Japanese), Morikita Publishing Co., Ltd. pp. 60–66 (2017).
[21] T. Hiroki et al., "Diagnosis of multiple cucumber infections with convolutional neural networks", IEEE Proc. AIPR, pp. 104 (2018).
[22] The National Agriculture and Food Research Organization, "Small Fruit Tree Manual (in Japanese)," (2018).
[23] Ministry of Health, Labour and Welfare, "Physical activity standards for health in 2013," pp. 51 (2013).
[24] M.H. Prio, F. Rios, "Kinematic Modeling of a Six Wheeled Differential Drive Intelligent Robot and Potential Field Method to Attain Obstacle Avoidance Capability," 2019 Southeast Con., pp. 1–4 (2019).
[25] N. Ito, N. Iguchi, "Steerability Control of Multi-Powered Wheel Vehicle," JSAM Journal, Vol. 50, No. 1, pp. 11–18 (1988).
[26] "How to plant fruit tree seedlings (in Japanese)",< https://minorasu.basf.co.jp/80083>, [referred Mar.2021].
[27] H. Iyatomi, "Trends and Challenges of Automatic Diagnosis Techniques for Plant Diseases," Neurology and Clinical Neuroscience, Vol. 26, No. 4, pp. 123–134, (2019).
[28] "PlantMD", <http://plant-md.org/>, [referred Oct 2021].
[29] The National Agriculture and Food Research Organization, "Small Fruit Tree Manual (in Japanese)", (2018).

(Received: October 30, 2021)
(Accepted: August 2, 2022)

Kenji Terada earned a B.E. degree from Polytechnic University, Tokyo and graduated from the course of Electrical Engineering and Computer Science, Graduate School of Engineering Polytechnic University. He is currently an Associate Professor of Polytechnic University, Tokyo. He received a Master's degree in Industrial Engineering from NIAD-UE Tokyo in 2002.

Masaki Endo earned a B.E. degree from Polytechnic University, Tokyo and graduated from the course of Electrical Engineering and Computer Science, Graduate School of Engineering Polytechnic University. He received an M.E. degree from NIAD-UE, Tokyo. He earned a Ph.D. Degree in Engineering from Tokyo Metropolitan University in 2016. He is currently an Associate Professor of Polytechnic University, Tokyo. His research interests include web services and web mining. He is also a member of DBSJ, NPO STI, IPSJ, and IEICE.

Takuo Kikuchi received a Ph.D. degree in Engineering from Kyushu Institute of Technology. He is currently a professor of the Dept. of Electrical and Computer Engineering at Polytechnic University. His research interests include "Information network cabling" and "Skill analysis and evaluations". He is a member of JSEE, IEICE, and JSET Japan.

Shigeyoshi Ohno earned M.Sci. and Dr. Sci. degrees from Kanazawa University and a Dr. Eng. degree from Tokyo Metropolitan University. He is currently a full Professor of Polytechnic University, Tokyo. His research interests include big data and web mining. He is a member of DBSJ, IPSJ, IEICE and JPS.

Submission Guidance

About IJIS

International Journal of Informatics Society (ISSN 1883-4566) is published in one volume of three issues a year. One should be a member of Informatics Society for the submission of the article at least. A submission article is reviewed at least two reviewer. The online version of the journal is available at the following site: http://www.infsoc.org.

Aims and Scope of Informatics Society

The evolution of informatics heralds a new information society. It provides more convenience to our life. Informatics and technologies have been integrated by various fields. For example, mathematics, linguistics, logics, engineering, and new fields will join it. Especially, we are continuing to maintain an awareness of informatics and communication convergence. Informatics Society is the organization that tries to develop informatics and technologies with this convergence. International Journal of Informatics Society (IJIS) is the journal of Informatics Society.

Areas of interest include, but are not limited to:

- Internet of Things (IoT)
- Smart Cities, Communities, and Spaces
- Big Data, Artificial Intelligence, and Data Science
- Network Systems and Protocols
- Computer Supported Cooperative Work and Groupware
- Security and Privacy in Information Systems
- Intelligent Transportation System
- Distributed Computing
- Multi-media communication
- Information systems
- Mobile computing
- Ubiquitous computing

Instruction to Authors

For detailed instructions please refer to the Authors Corner on our Web site, http://www.infsoc.org/.

Submission of manuscripts: There is no limitation of page count as full papers, each of which will be subject to a full review process. An electronic, PDF-based submission of papers is mandatory. Download and use the LaTeX2e or Microsoft Word sample IJIS formats.

http://www.infsoc.org/IJIS-Format.pdf

LaTeX2e

LaTeX2e files (ZIP) http://www.infsoc.org/template_IJIS.zip

Microsoft Word™

Sample document http://www.infsoc.org/sample_IJIS.doc

Please send the PDF file of your paper to secretariat@infsoc.org with the following information:

Title, Author: Name (Affiliation), Name (Affiliation), Corresponding Author. Address, Tel, Fax, E-mail:

Copyright

Publisher

Address: Informatics Laboratory, 3-41 Tsujimachi, Kitaku, Nagoya 462-0032, Japan

E-mail: secretariat@infsoc.org

CONTENTS